Resources, Conservation & Recycling 188 (2023) 106658

Contents lists available at ScienceDirect

Resources, Conservation & Recycling

journal homepage: www.elsevier.com/locate/resconrec

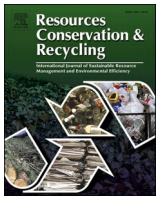

Full length article

Quantification of the food-water-energy nexus in urban green and blue infrastructure: A synthesis of the literature

Fanxin Meng [a], Qiuling Yuan [a], Rodrigo A Bellezoni [b], Jose A. Puppim de Oliveira [b,c,d], Silvio Cristiano [e], Aamir Mehmood Shah [a], Gengyuan Liu [a,f], Zhifeng Yang [a,g,*], Karen C. Seto [h]

[a] State Key Joint Laboratory of Environment Simulation and Pollution Control, School of Environment, Beijing Normal University, Beijing 100875, China
[b] São Paulo School of Management (FGV EAESP), Fundação Getúlio Vargas (FGV), Rua Itapeva, 474, sala 712, Bela Vista, São Paulo, 01332-000, Brazil
[c] Brazilian School of Public and Business Administration (FGV EBAPE), Fundação Getúlio Vargas (FGV), Rua Jornalista Orlando Dantas 30, Rio de Janeiro, Brazil
[d] Institute for Global Public Policy, Fudan University, Shanghai, China
[e] Department of Environmental Sciences, Informatics and Statistics, Università Ca' Foscari Venezia via Torino 155, 30172 Mestre, Venice, Italy
[f] Beijing Engineering Research Center for Watershed Environmental Restoration & Integrated Ecological Regulation, Beijing 100875, China
[g] Key Laboratory for City Cluster Environmental Safety and Green Development of the Ministry of Education, School of Ecology, Environment and Resources, Guangdong University of Technology, 510006 Guangzhou, China
[h] Yale School of the Environment, Yale University, 380 Edwards St, New Haven, CT, 06511, USA

ARTICLE INFO

Keywords:
Urban green and blue infrastructure
Trade-offs
Life cycle thinking
Food-water-energy nexus
Nature-based solutions

ABSTRACT

Green and blue infrastructure (GBI) is an innovative strategy to tackle food-water-energy (FWE) nexus issues. GBI can provide the benefits of food production, energy saving and generation, waterlogging control, rainwater cleansing and harvesting. Significant efforts have been devoted to measuring the implications of GBI on FWE nexus. However, there is little research to simulate the multiple linkages between GBI and FWE nexus in urban areas, and the lack of a unified methodology framework also easily leads to an understanding bias of their connections and makes it challenging to compare the results. Focusing on the prior published literature, this study clarifies the interactions between GBI and FWE nexus and reviews the methods to quantify the implications of GBI on FWE nexus in cities, including FWE-related benefits, life cycle environmental impacts, and avoided upstream environmental footprints induced by FWE-related benefits. It is revealed that most studies focus on the FWE-related benefits or (and) life cycle environmental impacts of GBI from a silo perspective. Researchers pay little attention to the avoided trans-boundary environmental footprints by GBI, and carbon footprint is the greatest concern in the existing research. There is little evidence on comprehensive quantifications regarding multiple impacts of GBI on FWE nexus at the urban scale. The review outlines methods to simulate the linkages between GBI and FWE nexus and calls for a holistic methodological framework to apply at the urban scale. Such assessment practices would make sense for FWE-oriented resilience planning and governance for urban GBI implementation.

1. Introduction

Projections suggest that 6.7 billion people, accounting for 67% of Earth's population will reside in urban areas by 2050 and it is estimated that 81% of the urban population will be in countries classified as developed by 2030 (United Nations, 2019). Despite socioeconomic benefits, augmenting urbanization leads to numerous problems, such as urban heat island (UHI) effects, risks of food shortages, and urban waterlogging events, threatening disruptions in food, water, and energy (FWE) domains in cities (Melo et al., 2020), which consequently results in challenges to urban resilience and regional sustainability (Fuhrman et al., 2020). At the same time, the intrinsic intersections between FWE resources, also referred to as the FWE nexus, further reshapes the shocks that were previously contained within a geographic area or a sector and are now becoming globally interconnected (Liu et al., 2018; Zhang et al., 2019), complicating the nexus issues posed to cities (Meng et al., 2019a; 2019b; 2022).

A holistic strategic planning approach known as green and blue infrastructure (GBI) delivers multiple FWE-related benefits from and to urban areas, such as food production, climate regulation, energy

* Corresponding author.
E-mail address: zfyang@bnu.edu.cn (Z. Yang).

https://doi.org/10.1016/j.resconrec.2022.106658
Received 7 March 2022; Received in revised form 19 August 2022; Accepted 9 September 2022
Available online 24 September 2022

savings, flood control, water purification, and rainwater harvesting (Elmqvist et al., 2013). This has significant impacts on urban FWE systems and ensures interconnection, versatility, and support for nature and ecosystems (Mell, 2017). Thus, GBI appears to be a good candidate for improving sustainability of urban systems. With the highlights of sustainable development goals (SDGs), food (SDG2), water (SDG6), and energy (SDG7), are targeted to achieve efficient water use, energy alternative, and agricultural practices (Biggs et al., 2015; Cristiano et al., 2021). In this context, GBI has become a powerful innovation to achieve the SDGs and compact the nexus challenges for urban resilience from the perspective of FWE nexus, through adaptive and flexible implementations (Hoyer et al., 2011; European Commission, 2013; Brink et al., 2016).

GBI consists of a diverse set of green infrastructures (e.g., urban forests, gardens, street trees, urban agriculture, green roofs, green walls) and blue infrastructures (e.g., water bodies, constructed wetlands, rain gardens, permeable pavements, bioswales) (Bellezoni et al., 2021). GBI elements can be woven into a community at several scales and implemented alone or associated with other GBIs. Previous studies classified different GBIs by categories and developed a conceptual framework of the critical links between urban GBI and FWE nexus, together with the direction and magnitude of the relationship. Specifically, GBI provides FWE-related benefits, such as food production, climate regulation, and water supply. As the increasing FWE demands can be satisfied locally, GBI also drives the reductions of emissions and consumptions embodied in the trans-boundary production and supply chains. However, GBI comes at the cost of capital, materials, and energy inputs. The environmental impacts in relation to these inputs are trade-offs for the FWE-related benefits that result from GBI (Bellezoni et al., 2021; Shah et al., 2021). For instance, urban agriculture increases the output of urban edible products in the operation stage and thereby reduces the environmental footprints embodied in the process of external food imports. Whereas during the entire life cycle stages, urban agriculture actuates environmental impacts in different pathways, such as energy input, water irrigation, and greenhouse gas emissions.

Such positive and negative impacts reflect the multiple linkages and trade-offs between urban GBI and FWE nexus, which need to be understood and evaluated within a specific local context and with a variety of stakeholders. Since the disservices of GBI are highly subjective and variable across different environments (Haase et al., 2014; 2017; Kremer et al., 2016), the comprehensive examination of GBIs' entire life cycle performances is necessary (Wang et al., 2020). Life cycle assessment (LCA) is a system analysis method that presents an opportunity to assess these trade-offs, compare designs, and choose the most appropriate GBI practices by quantifying a variety of environmental impacts and benefits (Spatari et al., 2011; Shafique et al., 2020). We here, therefore, underline the cardinal role of LCA to systematically capture the intrinsic connections between GBI and FWE nexus considering positive benefits and adverse impacts.

Currently, researchers are paying more attention to the linkages between GBI and FWE nexus. Cristiano et al. (2021) qualitatively reviewed the benefits and limitations of green roofs based on an integrated food-water-energy-ecosystem nexus approach, together with the SDGs. The authors reflected that most of the studies focused on a silo approach, but green roofs should be fully evaluated on the sustainable development of cities and communities through a nexus approach. Melo et al. (2021) established a hybrid framework for forests into a food-water-energy nexus approach, highlighting the critical promotion of forests in food, water, and energy security and societies to achieve SDGs. They also presented three key principles of the food-water-energy nexus: mainstreaming forest restoration, empowering local communities, and implementing nature-based solutions. Caputo et al. (2021) developed a conceptual methodology framework for measuring the resource efficiency, food production, motivations, and health benefits of urban agriculture from the perspective of food-water-energy-people nexus. The proposed framework comprised a combination of methods, such as urban agriculture logbooks, a database of urban agriculture activities, LCA, and material flow analysis, to allow the upscaling of the investigation results from a garden scale to the city scale.

Most of the prevailing quantitative research on GBI and FWE nexus is based on a single aspect, such as direct FWE-related benefits (Moody and Sailor, 2013; Orsini et al., 2014; Winston et al., 2016) or life cycle environmental impacts of GBI (Andrew and Vesely, 2008; Manso et al., 2018; Pushkar, 2019). Some research has further focused on the trade-offs analysis by comparing the positive benefits and adverse impacts of GBI (De Sousa et al., 2012; Wang et al., 2013; Moore and Hunt, 2013; Xu et al., 2021; Shah et al., 2022). More comprehensively, Toboso-Chavero et al. (2019) made a vital advance in measuring the effects of green roofs, including direct benefits (food production, energy generation, and rainwater harvesting), indirect avoidance of carbon emissions, and life cycle impacts at community scale. Despite significant contributions from these studies, there lacks a systematic method introduction to promote the quantification of relevant FWE implications regarding a broad set of GBI categories at the urban scale. Our starting point is to support embracing quantitative explorations to break the understanding obstacles of GBI and FWE nexus and the multiple interplays within them, as the quantitative results would be a cornerstone to guide stakeholders in FWE-oriented resilience planning and governance for urban GBI implementation. Therefore, to overcome the knowledge gaps, we identified the detailed interactions between GBI and FWE nexus and provided an overview of the available methods to quantify the FWE flows and trade-offs of GBI based on the methodological articles.

The rest of this paper is organized as follows: Section 2 outlines the process of review sample selection; Section 3 visualizes the inherent correlations between GBI and FWE nexus; Section 4 introduces the main methods for assessing the FWE-related benefits of GBI; and Section 5 reviews the trade-offs evaluation studies of GBI based on LCA. The conclusions and discussions are drawn in Section 6.

2. Review methodology

To make this literature review as comprehensive and detailed as possible, a wide range of relevant sources were examined to find published methodological articles. We determined a set of initial keywords according to the authors' expertise and iteratively optimized them through database searching. The retrieved keywords included four aspects: GBI categories, FWE-related topics, research boundaries, and quantitative evaluation. GBI categories were based on the typologies described by Bellezoni et al. (2021), including green roofs, green walls, street trees, constructed wetlands, urban forests, green spaces, urban agriculture, and so on. Typical search terms are available in the Supporting Information (see **Table S1)**. These keywords were then combined and connected to obtain the retrieval string; for instance, the following was used for the green roof-energy search: TS[1] = ("green roof" OR "roof greening" OR "roof greenery") AND TS = ("energy") AND TS = ("urban" OR "municipal" OR "city" OR "metropolitan" OR "neighbo*" OR "communit*") AND TS = ("model*" OR "method*" OR "quantif*" OR "approach" OR "simulat*" OR "estimat*" OR "evaluat*"). The literature search was performed in three databases, namely, Web of Science, ScienceDirect, and Google Scholar, and the principal language reference was English, with a restriction on the publication year from 1990 to March 2021 being applied. Our results are not fully comprehensive since relevant non-English language articles may exist. However, our search results that are in a fairly restrictive selection of papers are sufficient to provide an overview of the main methods used in the literature on GBI and FWE nexus.

By screening based on a series of pertinence and uniqueness principles (as reported in Fig. 1), a total of 456 articles were deemed suitable

[1] In Web of Science, TS stands for "Topic".

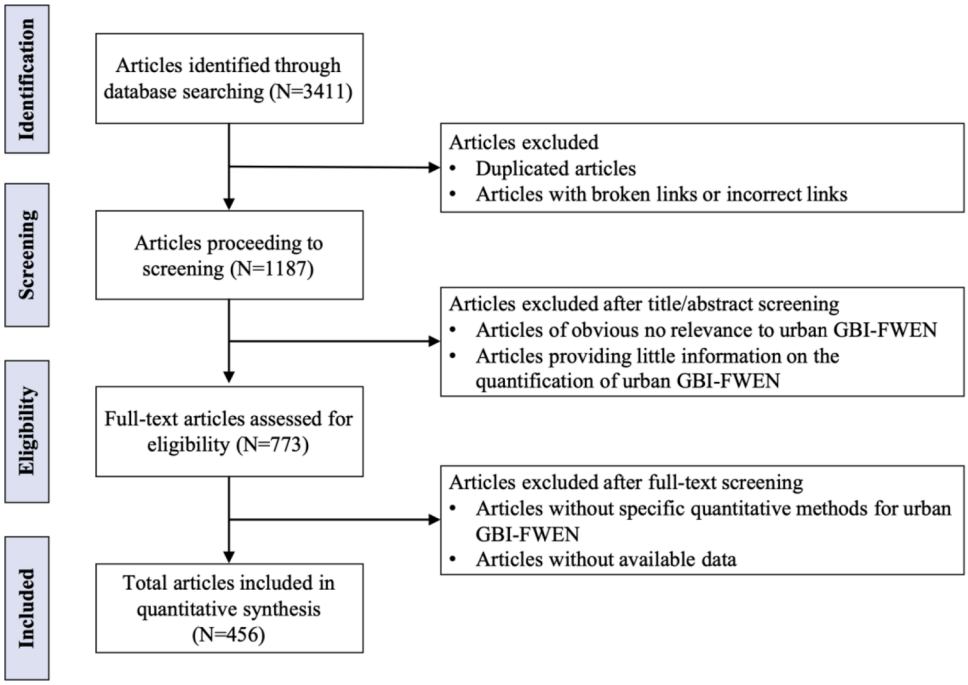

Fig. 1. Flowchart of literature selection and sample data collection.
Note: N represents the number of articles; GBI-FWEN is short for the linkages between GBI and FWE nexus.

for inclusion in this review. Fig. 1 shows the details of the literature selection and exclusion process.

3. Linkage identification between GBI and FWE nexus

In light of our review, as visualized in Fig. 2, some common aspects of the linkages between urban GBI and FWE nexus are highlighted. In previous research, we have identified the relationship between different types of GBI and FWE nexus (Bellezoni et al., 2021). Further, in this paper, we focus on the inherent correlations between GBI and FWE nexus to guide the quantification of their linkages. As shown in Fig. 2, GBI can offer great FWE-related benefits to the environment and human beings, such as local food production, temperature regulation (and their effects on the UHI reduction that ultimately causes energy savings), and water savings by rainwater harvesting. Since the demand for urban FWE resources decreased, the trans-boundary environmental footprints in the upstream production and supply chains would consequently be avoided. Certain applications of GBI, however, show specific negative impacts during whole life cycle processes, such as energy and water consumption and greenhouse gas emissions. Based on this, we attach significant importance to the quantification of both positive and negative impacts of GBI on FWE nexus. Therefore, the following sections of this study review the quantitative methods of FWE-related benefits and trade-off studies of GBI, which may provide an ideological basis for the linkage simulation between GBI and FWE nexus.

4. Quantification of the FWE-related impacts of urban GBI

This section aims to outline the quantitative methods of the implications of GBI in relation to FWE domains, including food (local food production), energy (climate regulation, energy saving, and energy generation), and water (runoff control, rainwater collection, and water purification), where provides the method introductions and specific cases, more details are presented in the following tables.

4.1. Food-related effects

GBI has become an increasingly popular farming system, as it provides space for urban agriculture and reshapes the edibility of GBIs and the local food-growing environment (Russo and Cirella, 2019). In recent years, the food production potential of urban gardens (McDougall et al., 2019; Caputo et al., 2021; Pourais et al., 2015), rooftop farms (Jing et al., 2020; Orsini et al., 2014; Sanyé-mengual et al., 2015), urban fruit trees (Lafontaine Messier et al., 2016; Grafius et al., 2020), and urban forests (McLain et al., 2012; Riolo, 2019) has been explored. Among the articles reviewed, rooftop farms are frequently studied at the building scale, and the tendency to gardens occurs at the community level. When considering large-scale farming, researchers prefer applying the concept of urban agriculture to discuss the total food production potential in cities more often, involving a variety of possible food cultivation spaces (building rooftops, gardens, farms, and arable land) (Clinton et al., 2018; Lee et al., 2015; Pulighe and Lupia, 2019; Sioen et al., 2017). In addition to predicting the food yield, the self-sufficiency of nutrients is measured as well because it can be understood as a realistic target for food produced and distributed within city boundaries. Potentially, micronutrient-rich foods (i.e., fruits and vegetables) are advocated for the limited amount of land in cities and the short supply chains to enhance food security (Weidner et al., 2019). This point also fits our findings in this paper; that is, most of the studies investigated the growing potential of vegetables or fruits, such as tomatoes, cabbage, grapes, and apples, which are easily planted in urban areas (Gondhalekar and Ramsauer, 2017; MacRae et al., 2010; Nadal et al., 2019). In this review, we identified three main quantitative approaches to estimate the local food production of urban GBIs, namely, (a) agricultural logbooks (AL), (b) statistical data (SD), and (c) model simulation (MS), applied either separately or in combination (see Table 1).

As the first-hand data of food production, the agricultural logbook is an essential means to determine the food productivity of urban GBI. McDougall et al. (2019) investigated 13 small-scale organic farms and gardens in Sydney according to the logbooks of gardening activities over the course of a year, and the results showed that the yield of 62 different vegetables, fruits, and herbs harvested in the plots reached an average

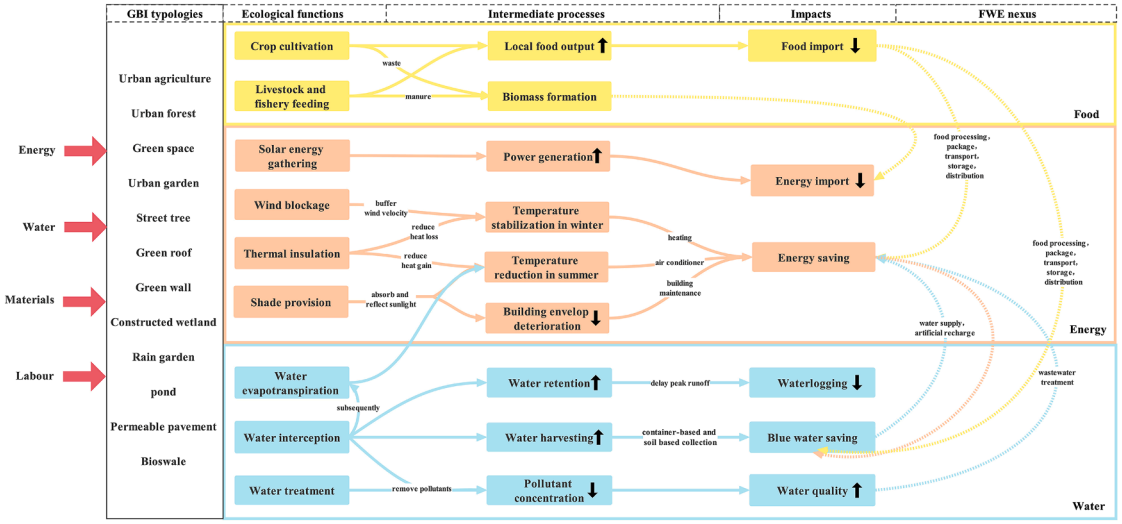

Fig. 2. Linkages between urban GBI and FWE nexus.
Note: Yellow: related to food; Orange: related to energy; Blue: related to water; Solid line: direct impacts; Dotted line: indirect impacts; Red arrow: energy and resource input; Up or down black arrow: increase or decrease trend; F-E: Food-Energy nexus; F-W: Food-Water nexus; E-W: Energy-Water nexus; W-E: Water-Energy nexus.

crop output of 5.9 kg/m^2. However, the workload for data collection is quite challenging because farmers and volunteers need to closely track the input and production of crops by recording data (Duchemin et al., 2008; Pourais et al., 2015; Sanjuan-Delmás et al., 2018). When it is difficult to obtain the first-hand data, the secondary statistical data sourced from national institutions or FAO[2] take a key part (MacRae et al., 2010; Lee et al., 2015; CoDyre et al., 2015). Sioen et al. (2017) estimated the vegetable yield and potential nutrients of urban agriculture based on the data from the 2015 Tokyo Metropolitan Agricultural Products Production Survey and found that the total vegetable production of professional farms was 4,776 tons, with an average nutritional self-sufficiency rate of 2.5%. Some standard online tools, such as Farming Concrete[3], Harvest Metre[4] and MyHarvest[5], also provide statistical data related to urban agriculture for reference. In addition, food yield prediction can be achieved through models such as DNDC[6], CityCrop[7], KASPRO[8], InVEST[9], and GAEZ[10]. These models are commonly used to quantitatively describe and forecast crop growth based on the internal growth law of crops and the causal relationship between crop genetic potential and environmental effects.

Overall, agricultural logbooks, statistical data, and model simulations are practical for estimating the food production of small-scale (such as building and community) edible GBIs. At the district, city, regional, and global scales, the prediction of agrarian yield usually requires two factors. One is to obtain the potential spatial area for urban agriculture development through spatial analysis (SA); researchers mainly use geographic information systems (GIS) and remote sensing (RS) technologies to identify the sites with potential for food production in the study area (Taylor and Lovell, 2012; Saha and Eckelman, 2017). The other is the crop yield per unit area, which is generally based on small-scale data (from national databases, FAO statistics, model simulation results, agricultural logbooks, or other literature data). Based on these two parameters, the urban agricultural output in the study area can be estimated. For instance, Pulighe and Lupia (2019) first used high-resolution Google Earth[11] images and ancillary data to map the potential urban agricultural area in Milan, Italy, and estimated the food productivity based on the data from the Ministry of Agriculture. The study reported that urban vegetable gardens could feed a population of 63,700 inhabitants, approximately 4.8% of the urban dwellers. Interestingly, with a productivity scenario of 5 kg/m^2 (similar to what McDougall et al. (2019) found in Sydney), the urban inhabitants' vegetable demands could be approximately satisfied within 2,000 hectares of vegetable garden space.

4.2. *Energy-related effects*

The implications of GBI on energy domains involve three aspects, which are respectively climate regulation, energy saving, and energy generation. The corresponding quantitative methods are introduced in the following three sub-topics. More details can be viewed from Tables 2-5.

(i) **Climate regulation**

By acting as urban heat sinks, vegetation and water bodies of GBI can effectively regulate the local microclimate and are therefore helpful for reducing the formation of UHIs. In addition, due to the wind blockage and thermal insulation of vegetation, greenery could also abate the heat loss in winter. To make a positive impact on urban climate, hydrology, and ecology, the evaluation of climate regulation benefits of GBI is necessary (Gaffin et al., 2012). In recent years, intensive research has been conducted to explore the impacts of GBIs on urban microclimates, involving green infrastructures, such as green roofs (Sendo et al., 2010; Lundholm et al., 2010), green wall/green facades (Cameron et al., 2014;

[2] The Food and Agriculture Organization of the United Nations (FAO): www.fao.org (retrieved on 25 November 2021)
[3] https://farmingconcrete.org (retrieved on 24 November 2021)
[4] https://www.capitalgrowth.org/the_harvestometer/(retrieved on 24 November 2021)
[5] https://myharvest.org.uk (retrieved on 24 November 2021)
[6] DeNitrification-DeComposition; https://www.globaldndc.net/ (retrieved on 24 November 2021)
[7] https://www.citycrop.io/ (retrieved on 24 November 2021)
[8] https://www.wur.nl/en/product/App-KASSIM-interactive-learning-tool-for-education-and-practice.htm (retrieved on 24 November 2021)
[9] Integrated Valuation of Ecosystem Services and Trade-offs https://naturalcapitalproject.stanford.edu/software/invest (retrieved on 24 November 2021)
[10] Global Agro-Ecological Zoning https://gaez.fao.org/ (retrieved on 24 November 2021)
[11] https://earth.google.com/web/ (retrieved on 24 November 2021)

Table 1
Methods review of food production by urban GBI.

Method	Spatial scale	GBI typology	Food-related Indicator	Empirical value	Reference
Lettuce yield	Model Simulation (MS: DNDC)	Building	Rooftop farm	Potato yield 11.7–25.5 kg/m^2/year	0.6–1.2 kg/m^2/year Jing et al., 2021
Agricultural Logbooks (AL)	Building	Rooftop farm (83.34 m^2)	Tomato yield	19.6 kg/m^2/year	Sanjuan-Delmás et al., 2018
	Community	Community garden (350 m^2)	Crop yield	1.3 kg/m^2/year	Caputo et al., 2021
	Community	Community garden (14.2 ha)	Vegetable yield	3.66 kg/m^2/year	Algert et al., 2014
	Community	Collective garden	Tomato yield	5.4 kg/m^2/year	Pourais et al., 2015
	Community	Collective garden	Vegetable yield	0.3–2.08 kg/m^2/year	Duchemin et al., 2008
	Community	Individual and community garden		2.4–5.4 kg/m^2/year	
	City	Urban garden (median plot area of 10.8 m^2)	Crop yield	5.94 kg/m^2/year	McDougall et al., 2019
Statistical Data (SD)	City	Urban agriculture (community gardens, market gardens, private gardens, and commercial farm)	Food and beverage self-sufficiency	4.2%–17.7%	Grewal and Grewal, 2012
Spatial Analysis & Agricultural Logbooks (SA + AL)	City	Rooftop farm (82 ha)	Vegetable yield (self-sufficiency rate)	15.2 kg/m^2/year (77%)	Orsini et al., 2014
	City	Vegetable garden (13.76 ha)	Vegetable yield	1.43 kg/m^2/year	CoDyre et al., 2015
Spatial Analysis & Statistical Data (SA + SD)	Neighborhood	Urban agriculture (168 ha of land)	Cabbage yield	9.16 kg/m^2/year	Gondhalekar and Ramsauer et al., 2017
			Apple yield	3.94 kg/m^2/year	
			Grape yield	1.14 kg/m^2/year	
	Ward	Urban agriculture (14.7 ha of hobby farms)	Total vegetable production (nutritional self-sufficiency rate)	884 ton/year (0.38%)	Sioen et al., 2017
		Urban agriculture (180.2 ha of professional farms)		4,776 ton/year (2.48%)	
	City	Urban agriculture (486.4 ha of public land and 136.4 ha of private land)	Vegetable yield	2.24 kg/m^2/year (conventional)	McClintock et al., 2013
				3.36 kg/m^2/year (low-biointensive)	
				5.6 kg/m^2/year (medium-biointensive)	
	City	Vegetable garden (98 ha)	Feed population	63,700	Pulighe and Lupia, 2019
			Vegetable yield	2.5 kg/m^2/year (conventional)	
				5 kg/m^2/year (medium management)	
		Urban agriculture (2,539 ha of arable land)	Maize yield	1.2 kg/m^2/year	
			Wheat yield	0.6 kg/m^2/year	
	City	Urban agriculture (5,115 ha of land)	Crop yield	1.22–9.54 kg/m^2/year	Lee et al., 2015
	City	Community garden (121,400 ha)	Vegetable yield	0.26 kg/m^2/year	Hara et al., 2018
		Urban agriculture (190,500 ha of remaining rice and dry fields)	Vegetable yield	5.12 kg/m^2/year	
			Rice yield	0.5 kg/m^2/year	
	Worldwide	Urban agriculture (rooftop farms, vertical farms, and vacant land)	Total potential grain production	100–180 million ton/year	Clinton et al., 2018

Pérez et al., 2017), urban parks (Monteiro et al., 2016), gardens (Xue et al., 2019), street trees (Shashua bar et al., 2011; Wang and Akbari, 2016), lawns (Snir et al., 2016), and blue infrastructures, such as water bodies (Yu et al., 2020) and constructed wetlands (Xue et al., 2019).

Modern urban landscapes feature a compact city form and augmenting UHI effects, leaving limited land resources for urban greening. Green roofs and green walls where vegetation is transplanted onto building rooftops and envelopes have shown effectiveness in providing environmental benefits to the cityscape through microclimate regulation, and serve as alternatives to traditional landscapes (Wong et al., 2021). A growing number of studies emerge to quantify the impacts of building greenery on urban microclimate basically according to temperature variations (air temperature, internal and external surface temperature at vegetation cover, building façade, indoor temperature, and land surface temperature). These papers tend to compare the indoor and outdoor temperatures of green roofs, cool roofs, traditional roofs (He et al., 2020; Ouldboukhitine et al., 2014), green walls and bare concrete walls (Sanchez-Resendiz et al., 2018; Wong et al., 2009), and green roofs and green walls (Alexandri and Jones, 2008) and investigate the thermal performance variations of different kinds of vegetation (Koyama et al., 2015; Zhang et al., 2020). In this review, we identified three approaches to quantify the climate regulation benefits of GBI: (a) field measurement (experimental and observational studies (EO)), (b) statistical modelling (SM), and (c) model simulation (MS). The quantitative methods and results of the climate regulation benefits of GBI are shown in Table 2.

Field measurements are usually carried out through the temperature monitoring of existing GBIs or specially built GBI test platforms. For example, Fioretti et al. (2010) examined the thermal performance of green roofs in the main building of Marche Polytechnic University by monitoring the meteorological parameters on site. A temperature reduction of nearly 6°C on green roofs compared to conventional roofs was obeserved. When there is no existing GBI for field measurements and the research scope exceeds the experimental scale, statistical modelling is usually taken to predict the temperature regulation benefits of GBI, such as the Monte Carlo approach, variance analysis, Pearson correlation analysis, and linear regression analysis. One example is the study by Dong et al. (2020), who explored the correlations between roof greening area and land surface temperature (LST) on Xiamen Island based on the RS data from Landsat. The results showed that the average LST difference between green roofs and Xiamen Island decreased by 0.91°C, and the average LST of the roof and its characteristic cooling buffer zone decreased by 0.4°C for every 1000 m^2 increase in roof greening area. However, landscape heterogeneity within cities may have

Table 2
Methods review of climate regulation by urban GBI.

Method	Spatial scale	GBI typology	Energy-related Indicator	Empirical value	Reference
Experimental and Observational Studies (EO)	Building	Green roof (0.25 m^2)	Air temperature reduction	0.8–3°C	Zhang et al., 2020
	Building	Green wall (5.46 m^2)	Indoor temperature reduction	2°C	Sánchez-Reséndiz et al., 2018
Experimental and Observational Studies & Statistical Modelling (EO + SM)	Site	Green wall	Wall surface temperature increase (in winter)	3°C	Cameron et al., 2015
	Building	Green wall (1.55 m^2)	Wall surface temperature reduction (maximum)	7°C	Blanco et al., 2019
	Top of a railway station	Extensive green roof (484 m^2)	Air temperature reduction	0.1–1.6°C	Peng and Jim, 2013
		Intensive green roof (484 m^2)		0.2–2.1°C	
	Building	Green wall	Indoor temperature reduction	3.94–4.89°C	Rupasinghe and Halwatura, 2020
	Building	Street tree	Wall surface temperature reduction	9°C	Berry et al. 2013
			Air temperature reduction	1°C	
Observational Studies & Statistical Modelling (OS + SM)	Block (5 ha)	Green space	Air temperature reduction	0.27°C	Park et al., 2017
	Block (9.8 ha)			0.63°C	
	Block (11 ha)			1.93°C	
Spatial Analysis & Experimental and Observational Studies & Statistical Modelling (SA + EO + SM)	Neighborhood (200×200×80 m)	Green wall (189.6 m^2)	Air temperature reduction	0.19–0.23°C	Peng et al., 2020
Spatial Analysis & Model Simulation (SA + MS: ENVI-met)	Building	Green roof (1,000 m^2)	Air temperature reduction	0.4–2.0°C	Berardi, 2016
	Residential area (300×300 m)	Street tree	Air temperature reduction	2–4°C	Wang and Akbari, 2016
Spatial Analysis & Model Simulation (SA + MS: WRF)	City (700 km^2)	Green roof	Air temperature reduction	2–3°C	Arghavani et al., 2020
Spatial Analysis & Model Simulation (SA + MS: MUKLIMO_3)	City (415.72 km^2)	Green roof (23.58 km^2)	Air temperature reduction	0.25–0.5°C	Žuvela-Aloise et al., 2018
Spatial Analysis & Statistical Modelling (SA + SM)	Garden (0.2–0.3 ha)	Green space	Air temperature reduction	0.3°C	Monteiro et al., 2016
	Square (0.8–3.8 ha)			0.4–0.8°C	
	Park (10.1–12.1 ha)			0.6–1.0°C	
	District	Green roof (0.65 km^2)	Land surface temperature reduction	1°C	Todeschi et al., 2020
	Island (142 km^2)	Green roof (0.54 km^2)	Land surface temperature reduction	0.4°C/1,000 m^2	Dong et al., 2020
	Reservoir, garden, park, river, lake (2.1–2,090.5 ha)	Constructed wetland	Air temperature reduction	2.74°C	Xue et al., 2019

impacts on the climate regulation benefits of GBI, and there are potential interactions between urban grey infrastructure and GBI. Ziter et al. (2019) underlined the specific synergies between urban grey infrastructure and GBI in climate adaptation. By fitting the relationship between tree canopy cover, impervious surface cover, and air temperature, the research suggested that nearly half of impervious surfaces and more than 40% of the canopy cover in the city was the most effective strategy to enhance temperature regulation services.

In addition, model simulations are extensively used by most studies; models such as ENVI-met[12] (Peng et al., 2020; Zhu et al., 2021; Wang and Akbari, 2016), WRF[13] (Arghavani et al., 2020; Huang et al., 2019; Yang and Bou-Zeid, 2019) and MUKLIMO_3[14] (Žuvela-Aloise et al., 2016; Žuvela-Aloise et al., 2018) are widely used to predict the air-plant-surface temperature as well as the land surface temperature, and simulate the temperature changes in different greening scenarios at multiple scales.

In conclusion, the climate regulation benefits of small-scale GBIs can be evaluated by field measurements and model simulations. For the quantitative evaluation at the scales of community, district, and city, it is often necessary to extrapolate the climate regulation benefits of GBI at a small scale. The first step is to obtain the surface climate parameters through geospatial analysis, analyse the relationship between the surface temperature and GBI vegetation coverage through statistical modelling, and then predict the temperature within the research scale. Additionally, considering varying factors such as time step, solar reflectivity and relative humidity, a number of researchers preferred running models , which is not only suitable for the simulation of temperature changes at the microscale but also widely used for large-scale temperature prediction (i.e., the urban and regional scales) (Koc et al., 2018).

(ii) **Energy saving potential**

GBI promotes cooling effects by providing shades and enhancing evapotranspiration in summer (Wong et al., 2021) and stabilizes indoor temperature by providing wind barriers and thermal insulation in winter (Pitman et al., 2015), thus regulating the indoor temperature and reducing the energy consumption of air conditioning and heating inside buildings. In urban areas, buildings consume a considerable amount of energy, and the demand for ventilation and air conditioning particularly comprise a large part of the electricity bills (Pan and Chu, 2016). Therefore, the energy saving characteristics of GBI could serve as a solution for urban energy consumption. Current quantitative research on GBI energy savings mostly focuses on the scale of buildings, such as

[12] https://www.envi-met.com/zh-hans/ (retrieved on 25 November 2021)
[13] Weather Research and Forecasting Model; https://ral.ucar.edu/solutions/products/weather-research-and-forecasting-model-wrf (retrieved on 25 November 2021)
[14] https://www.dwd.de/EN/ourservices/muklimo_thermodynamic/muklimo_thermodynamic.html (retrieved on 25 November 2021)

green roofs above building rooftops and green walls on building envelopes, and quantifies their effects in summer (Akbari et al., 1997; Kong et al., 2016; Pan and Chu, 2016; Peng and Jim, 2015). However, relatively few articles have explored the winter thermal effect and heating energy saving potential of GBIs (Coma et al., 2017; Djedjig et al., 2017; Xing et al., 2019) since there has been controversy over the thermal performance of GBIs in winter. Some studies have demonstrated their negligible energy benefits and even increased the heating load of buildings in winter, due to the limited capacity to store and transmit heat downwards to indoor spaces (Theodosiou et al., 2014; Lee and Jim, 2020). Given that much of the energy consumed in cities is generated outside their city boundaries, it is of great significance to evaluate the energy saving potential of GBI for urban and regional energy planning. From this review, we identified three main approaches to evaluate the energy saving potential of urban GBIs: (a) field measurement (experimental and observational studies (EO), experimental studies (ES), observational studies (OS)), (b) model simulation (MS), and (c) temperature-energy empirical formulas (TE). The quantitative methods and results of energy savings of GBI are shown in Table 3.

The energy saving benefits of GBIs can be estimated through field measurements; that is, researchers install on-site monitors to measure the power required for heating and air conditioning and estimate the building energy saving potential after the implementation of a given GBI (Xing et al., 2019; Campos-Osorio et al., 2020; Cameron et al., 2015). The energy saving benefits of small-scale GBIs can also be quantitatively estimated by model simulations, such as EnergyPlus[15], Design Builder[16], and TRNSYS[17]. Moody and Sailor (2013) used EnergyPlus to evaluate the dynamic thermal performance of green roofs in a three-story office building. Their simulation results of Portland, Oregon and Houston, Texas showed that approximately 2% of the energy saving benefits of heating and fans in winter could be achieved when implementing green roofs in these two cities.

In addition, the temperature-energy empirical formula is applicable for energy saving evaluation because direct relationships exist between temperature and energy (Moreno, 2011). The temperature change of GBI's surrounding environment is first required through field measurement or model simulation; then, according to the temperature-energy empirical formula, the energy consumption (Q) of building heating and air conditioning can be calculated. The typical formula $Q=T\times h\times A$ considers the temperature difference (T), heat transfer coefficient of the matrix material (h, depending on the heat transfer of the GBI matrix material), and the area of GBI (A). In addition, the formula $Q=T\times c\times m$ is applicable, which considers the temperature difference (T), air-specific heat capacity (c), and air weight (m).

On balance, the energy saving potential of a small-scale GBI can be quantified by field measurements, empirical formulas, and model simulations. Nevertheless, the model simulation approach is more applicable than the other two methods because of its high prediction accuracy (51.2% of the reviewed studies use simulation models). When quantifying the energy saving potential of GBIs at a district or urban scale, it is usually extrapolated based on the energy savings of small-scale GBIs (Todeschi et al., 2020). The first step is to determine the potential area of GBI implementation by GIS within the study area and then to multiply the potential area of GBI with the energy savings value per unit area of small-scale GBI, to realize an estimation of the total energy savings of GBI by scaling up.

(iii) **Energy production potential**

GBI could contribute to urban energy production directly by bioenergy utilization and improve energy generation efficiency through solar photovoltaic panels installed on green roofs. The evaluation methods and results of the energy production of GBI are shown in Table 4 and Table 5.

(1) **Bioenergy production evaluation**

The vegetation and waste of urban GBIs serve as important bioenergy sources. Making use of bioenergy can help meet the energy demand of some cities and alleviate the pressure on energy supplies, since bioenergy would occupy an increasing share in the future energy scenario (IPCC, 2014). Studies have been conducted to evaluate the bioenergy potential of GBIs, such as constructed wetlands (Liu et al., 2019; Wang et al., 2011; Avellán and Gremillion, 2019), urban forests (Kraxner et al., 2016), green spaces (Springer, 2012), green roofs (Astee and Kishnani, 2010), urban parks (Shi et al., 2013) and street trees (Nurmatov et al., 2016). The reviewed studies identified two approaches to quantify the bioenergy potential of GBI: (a) field measurement (experimental and observational studies (EO), experimental studies (ES), observational studies (OS)), and (b) statistical modelling (SM).

To estimate the vegetation biomass of a small-scale GBI, experimental measurements are often used. Researchers collected vegetation samples in the field, weighed the fresh weight in the laboratory, and dried the samples to a constant weight; then, they measured the dry weight and analysed the sample area as well as the sample biomass data. Finally, the vegetation biomass of GBI within the research scope can be estimated. Based on field measurements, Liu et al. (2019) assessed the plant biomass in a constructed wetland in Zhejiang, China. They initially divided a constructed wetland of 1,000 m^2 into 12 plots of 2.0×2.5 m, cut and sorted the harvested plant by species in a single plot; then, they measured the biomass in plants in the laboratory and found that the average biomass of plants collected was 37,813 dry weight kg/ha/year.

Note that field measurements lead to high-accuracy results, but the experimental processes used are typically cumbersome, and field measurements are more applicable for evaluating the vegetation biomass of small-scale GBIs. For large-scale GBIs (such as cities), statistical modelling is preferred. The first step is to obtain the vegetation information in the study area through spatial analysis, such as vegetation types and the proportion of vegetal species. The second step is to analyse the correlations between vegetation information and biomass values for the prediction of bioenergy potential of GBI vegetation within study areas. Kraxner et al. (2016) simulated the possible biomass of the Vienna forest through statistical modelling. They first divided the urban forest area through geospatial analysis, then analysed the proportion of different tree species in the study area, and concluded that the annual biomass yield within a 4,200-ha forest area in Vienna was 13,000 t by modelling the theoretical biomass potential of the forest based on the biophysical growth and yield of a single tree species.

(2) **Photovoltaic (PV) output evaluation on green roofs**

According to research from Cavadini and Cook (2021), green roofs increase the annual power generation of PV panels by an average of 1.8% compared with traditional roofs. The main reason is that green roofs can help stablize the temperature of photovoltaic modules in a lower range and thus effectively increase the generation efficiency of photovoltaic power. In this review, we identified four approaches to quantify PV output: (a) field measurement (experimental and observational studies (EO), experimental studies (ES), observational studies (OS)), (b) statistical modelling (SM), (c) solar-power empirical formulas (SP), and (d) model simulation (MS).

The power generation of PV panels can be obtained according to the field measurement value; that is, researchers install electronic power recorders (such as micro inverters) to measure the output of PV panels and estimate the power generation potential. It is also feasible to predict large-area green roof PV power generation by fitting the relationship

[15] https://energyplus.net/ (retrieved on 25 November 2021)
[16] https://designbuilder.co.uk/ (retrieved on 25 November 2021)
[17] Transient System Simulation Tool; http://www.trnsys.com/ (retrieved on 25 November 2021)

Table 3
Methods review of energy saving by urban GBI.

Method	Spatial scale	GBI typology	Energy-related Indicator	Empirical value	Reference
Experimental and Observational Studies (EO)	Building	Green wall (8.22 m^2)	Cooling energy saving in sunny days (rate)	0.16 kWh/m^2/day (18.3%)	Pan and Chu, 2016
			Cooling energy saving in cloudy days (rate)	0.1 kWh/m^2/day (14.0%)	
			Cooling energy saving in rainy days (rate)	0.09 kWh/m^2/day (13.6%)	
	Building (experimental room, 0.2×0.1×0.07 m)	Green wall	Heating energy saving rate	21%–37%	Cameron et al., 2015
	Building (experimental room, 2.4×2.4×2.4 m)	Green wall	Cooling energy saving rate	34%	Pérez et al., 2017
	Building	Green wall (38 m^2)	Heat flux reduction rate	49%	Campos-Osorio et al., 2020
Experimental and Observational Studies & Temperature-Energy Empirical Formulas (EO + TE)	Building (experimental room, 3×2.5×3 m)	Green roof & green wall	Heating energy saving in winter (rate)	0.07 kWh/m^2/day (18%)	Xing et al., 2019
Experimental and Observational Studies & Temperature-Energy Empirical Formulas & Model Simulation (EO + TE + MS: ENVI-met)	District (6.7 km^2)	Extensive green roof (120.4 ha)	Cooling energy saving in summer (rate)	57.6 kWh/m^2 (14%)	Peng and Jim, 2015
		Intensive green roof (120.4 ha)		80.6 kWh/m^2 (23%)	
Temperature-Energy Empirical Formulas & Model Simulation (TE + MS: ENVI-met)	Block (100×200 m)	Green wall	Cooling energy saving rate	6%–20%	Li et al., 2018
Spatial Analysis & Observational Studies & Model Simulation (SA + OS + MS: EnergyPlus)	Building	Green wall (189.6 m^2)	Cooling energy saving (rate)	0.12–0.35 kWh/m^2/day (3.2%–11%)	Peng et al., 2020
			Cooling energy saving in summer	11–31 kWh/m^2	
Spatial Analysis & Temperature-Energy Empirical Formulas & Statistical Modelling (SA + TE + SM)	District	Green roof (64,712 m^2)	Heating energy saving	88 kWh/m^2/year	Todeschi et al., 2020
			Cooling energy saving	10 kWh/m^2/year	
Spatial Analysis & Model Simulation (SA + MS: EnergyPlus)	Building	Green roof (1000 m^2)	Cooling and heating energy saving (rate)	10 kWh/m^2/year (3%)	Berardi, 2016
Model Simulation (MS: Design Builder, TRNSYS)	Building (37 m^2 of house)	Green wall	Cooling energy saving	2.8–13.6 kWh/m^2/year	Dabaieh and Serageldin, 2020
			Heating energy saving	7.9–16 kWh/m^2/year	

Table 4
Methods review of bioenergy production by urban GBI.

Method	Spatial scale	GBI typology	Energy-related Indicator	Empirical value	Reference
Experimental Studies & Statistical Modelling (ES + SM)	Site	Constructed wetland (0.1 ha)	Biomass yield	37.8 ton/ha/year	Liu et al., 2019
	City	Green space (3,150 ha)	Biomass yield	1.2 ton/ha/year (normal rainfall scenario)	Springer, 2012
			Biomass yield	2 ton/ha/year (high rainfall scenario)	
Spatial Analysis & Observational Studies & Statistical Modelling (SA + OS + SM)	Basin	Constructed wetland (3.29 ha)	Biomass yield	5.1 ton/ha/year	Wang et al., 2011
Spatial Analysis & Statistical Modelling (SA + SM)	City	Urban forest (4,200 ha)	Biomass yield	3.1 ton/ha/year	Kraxner et al., 2016

between PV panel temperature and measured power output (Nagengast et al., 2013). In addition, there are studies calculating PV power generation directly based on the solar-power empirical formula, which mainly considers the solar radiation, photovoltaic array area, PV module conversion efficiency, etc. Jahanfar et al. (2018) used the solar energy-electricity empirical formula $PE_{PV}=3.6\times I_{solar}\times\varphi\times PR_T$ to calculate the power generation of PV panels in green roofs per unit area, where PE_{PV} is the PV power generation, 3.6 is the conversion coefficient (MJ/kWh), I_{solar} is the solar radiation received by PV panels per unit area, φ is the conversion efficiency of PV modules, and PR_T is the temperature performance ratio of PV modules (which decreases with increasing temperature). In addition, model simulations, including EnergyPlus, PVsyst[18], SAM[19], etc., are often used for PV power generation simulations under scenario analysis.

4.3. Water-related effects

The popular knowledge is that GBI can shape healthy water

[18] https://www.pvsyst.com/ (retrieved on 25 November 2021)
[19] https://sam.nrel.gov/ (retrieved on 25 November 2021)

Table 5
Methods review of PV output by urban green roof.

Method	Spatial scale	GBI typology	Energy-related Indicator	Empirical value	Reference
Experimental and Observational Studies & Model Simulation (EO + SM)	Building	Green roof (123 m^2, installed with 60 PV panels)	PV power generation	94–213 kWh/m^2/year	Nagengast et al., 2013
Experimental and Observational Studies & Model Simulation (EO + MS: PVsyst)	Building	Green roof (installed with PV panels of 10 m^2)	Specific PV power generation	33.6 kWh/m^2/year	Baumann et al., 2019
Model Simulation (MS: EnergyPlus)	Building	Green roof (29–549 m^2, installed with PV panels)	PV power generation	81–83 kWh/m^2/year	Zheng and Weng, 2020
Solar-Power Empirical Formulas & Statistical Modelling (SP + SM)	City	Green roof (2000 m^2, installed with PV panels)	PV power generation	183–206 kWh/m^2/year	Jahanfar et al., 2018
Observational Studies & Model Simulation (OS + MS: SAM)	Nationwide	Green roof (525 m^2, installed with 156 PV panels)	Annual increased PV power generation rate compared with traditional photovoltaic roof	1.8%	Cavadini and Cook, 2021

environments in urban areas, generally through runoff regulation, rainwater collection, and water purification. Here we stated these three corresponding quantitative methods of the water-related effects of GBI and listed key information in Tables 6-8.

(i) Runoff regulation

GBI systems have been widely implemented in urban areas to delay urban peak runoff and prevent waterlogging with the functions of detention, infiltration, and evapotranspiration (Lund et al., 2019). The runoff reduction capacity of GBI is closely related to the magnitude of storm events, including event duration and peak flow intensity. Among the relevant studies, green roofs, bioretention cells, and permeable pavements accounted for large proportions of the studied subjects. In particular, the stormwater control performance for single GBI facilities at the site scale was reflected to be limited, especially during higher intensity storm events (Li et al., 2018). Therefore, the past years have exhibited a trend towards a mixture of decentralized elements, and concepts such as sponge cities and low-impact development facilities that integrate various GBIs at various scales (i.e., community, cities and regions) are gaining popularity in the area of urban water management (Eckart et al., 2017; Chan et al., 2021). In this review, we identified three approaches to quantify the runoff regulation effects of GBI: (a) field measurement (experimental studies (ES), observational studies (OS)), (b) statistical modelling (SM), and (c) model simulation (MS). The quantitative methods and results of runoff regulation of GBI are shown in Table 6.

The runoff regulation capacity of GBI can be estimated using field experiments, that is, by installing rainfall equipment (such as rain gauges, rainfall simulators, hydraulic pipes, and rainwater collection pipes) at existing field sites or newly-built test beds. According to the measured runoff data (such as cumulative rainfall, rainfall intensity, humidity, soil water content, rainwater retention volume, matrix volume retention rate, return period, lag time, and runoff reduction rate), the runoff regulation capacity of GBI can be evaluated. Bortolini et al. (2020) built a green roof experimental platform (composed of 36 micro vegetation modules) at the University of Padua, Italy, and evaluated the rainwater retention capacity of green roofs by recording parameters, such as temperature, rainfall, and outflow of the micro modules. The results showed that during a two-year study period, the rainwater retention of roof vegetation for rainfall events less than 10 mm was 100% and those for rainfall events of 10–25 mm and higher than 25 mm were 48%–95% and 20%–88%, respectively.

However, the sampling data of field measurements are limited because of the demanding long-term monitoring and small application scale. Alternatively, model simulation can be used to evaluate the runoff regulation effects of GBI at various scales, and the commonly used models are SWMM[20] (Yao et al., 2020; Alihan et al., 2018), HYDRAUS[21] (Feitosa and Wilkinson, 2016), MIKE[22] (Khurelbaatar et al., 2021), SWAT[23] (Giese et al., 2019), HEC-RAS[24] (Ertan and Celik, 2021), Rutter[25] (Gonzalez-Sosa et al., 2017), and i-Tree[26] (Song et al., 2020). SWMM, MIKE, SWAT, HEC-RAS, and Rutter are suitable for multiscale assessment, while HYDRAUS and i-Tree are frequently applied to small-scale simulations with high accuracies, such as the prediction of the runoff reduction rate of permeable pavements and green roofs (Bouzouidja et al., 2018; Bautista and Peña-Guzmán, 2019). Jung et al. (2014) quantified the runoff regulation benefits of a constructed wetland in South Korea based on the HEC-RAS model. The results showed that the maximum flood level decreased by 0.81 m after completing the constructed wetland. The total inundation area fell by approximately 1.99 km^2, reporting that the constructed wetland had significant runoff regulation effects.

(ii) Rainwater collection

The rainwater collection means of GBI are divided into container-based and soil-based rainwater collections in this review. Direct rainwater collection can be realized by combining GBI with water storage devices, such as reservoirs and water storage tanks (e.g., setting rainwater collection tanks on green roofs), and the collected rainwater is usually used as irrigation water or other nondrinking water . Such container-based rainwater collection capacity relates to local precipitation regime (i.e., the precipitated volumes and their temporal variability), storage capacity of containers, and availability of GBI surfaces (Campisano and Modica, 2014). Moreover, through soil infiltration, runoff from the surface of the ground-based GBI can be filtered through the unsaturated zone of soils and then enter the groundwater. In addition to recharging groundwater, part of the rainwater can be stored in the natural water storage space (such as constructed wetlands). These

[20] Storm Water Management Model; https://www.epa.gov/water-research/storm-water-management-model-swmm (retrieved on 25 November 2021)
[21] https://www.pc-progress.com/en/default.aspx?hydrus-3d (retrieved on 25 November 2021)
[22] https://www.mikepoweredbydhi.com/ (retrieved on 25 November 2021)
[23] The Soil & Water Assessment Tool; https://swat.tamu.edu/ (retrieved on 25 November 2021)
[24] Hydrologic Engineering Center's River Analysis System; https://www.hec.usace.army.mil/software/hec-ras/ (retrieved on 25 November 2021)
[25] The Rutter model was constructed by Rutter et al. (1971); https://doi.org/10.1016/0002-1571(71)90034-3 (retrieved on 25 November 2021)
[26] https://www.itreetools.org/tools/i-tree-eco (retrieved on 25 November 2021)

Table 6
Methods review of runoff regulation by urban GBI.

Method	Spatial scale	GBI typology	Water-related Indicator	Empirical value	Reference
Experimental Studies & Statistical Modelling (ES + SM)	Building	Green roof (1150 m^2)	Runoff volume reduction rate	5%–69%	Bliss et al., 2009
	Building	Green roof (test bed, 3 m^2)	Runoff volume reduction rate	0.04%–99.95%	Stovin et al., 2012
			Lag time (minute)	4.5–231	
	Roadway (54.8 m^2)	Bioretention cell	Runoff volume reduction rate	32.7%–84.3%	Lucke and Nichols, 2015
	Campus and garden	Bioretention cell (182 m^2)	Runoff volume reduction rate	36%–59%	Winston et al., 2016
			Peak flow reduction rate	24%–96%	
	Parking lot	Bioretention cell	Runoff volume reduction rate	63%–89%	Brown and Hunt, 2012
			Peak flow reduction rate	84%-95%	
	Parking lot	Permeable pavement (108 m^2)	Runoff volume reduction rate	91.1%–100%	Collins et al., 2008
			Peak flow reduction rate	12.5%–100%	
			Lag time (minute)	28–50	
	Parking lot	Bioretention cell (35 m^2)	Runoff volume reduction rate	97%	DeBusk and Wynn, 2011
	Building	Green roof (test bed, 0.2 m^2)	Peak flow reduction rate	91%–99%	Kuoppamäki et al., 2016
Experimental Studies & Model Simulation (ES + MS: HYDRAUS)	Building	Green roof (37 m^2)	Runoff volume reduction rate	21.6%–100%	Hilten et al., 2008
			Peak flow reduction rate	0.4%–100%	
			Lag time (minute)	264–336	
Experimental Studies & Model Simulation (ES + MS: SWMM)	Hill town (11.75 km^2)	Greenbelt	Runoff volume reduction rate (one year)	52.5%–57.3%	Luan et al., 2017
		Permeable pavement		7.3%–12.2%	
		Bioretention		12.1%	
		Vegetative swale		3%	
Experimental Studies & Model Simulation (ES + MS: SLAMM)	Parking lot (881.6 m^2)	Permeable pavement (209 m^2)	Runoff volume reduction rate	80%	Mahmoud et al., 2020
Observational Studies & Water Balance Equation & Model Simulation (OS + WBE + MS: SWMM)	City	Green roof (1000 m^2), bioretention cell (50 m^2), detention basin	Runoff volume reduction rate	54%–85%	Kristvik et al., 2019
Experimental Studies & Water Balance Equation & Statistical Modelling (ES + WBE + SM)	Building	Green roof (test bed, 0.36 m^2)	Runoff volume reduction rate	60%	Harper et al., 2015
Model Simulation (MS: MIKE)	Region (28.1 km^2)	Bioretention cell, permeable pavement, green roof (with total area of 1.04 km^2)	Runoff volume reduction rate	64.0%–81.5%	Li et al., 2018
			Peak flow reduction rate	0–69.1%	
			Lag time (minute)	0–48	
Model Simulation (MS: self-developed model)	Community (0.55 km^2)	Green space (50% conversion)	Runoff volume reduction rate	13.3%–23.6%	Liu et al., 2014
			Peak flow reduction rate	1.3%–5.6%	
		Permeable pavement (50% conversion)	Runoff volume reduction rate	42%–46.2%	
			Peak flow reduction rate	35.7%–37.9%	
Spatial Analysis & Model Simulation (SA + MS: L-THIA LID)	Building, street, parking lot Watershed	Green roof, permeable pavement	Runoff volume reduction rate	23%–42%	Eaton, 2018
				35%–55%	

two kinds of soil-based flows (groundwater recharge and natural rainwater storage) through GBI are regarded as indirect means of rainwater collection. The review identified four approaches to quantifying the rainwater collection amount: (a) empirical formulas (EF), (b) water balance equations (WBE), (c) model simulation (MS), and (d) physical method (PM), including water table fluctuation method and soil conservation service curve number model (SCS-CN)[27]. The quantitative methods and results of the rainwater collection of GBI are shown in Table 7.

To estimate the direct rainwater collection amount of GBI, the empirical formula RH=A×P×C is applicable for multiscale estimation, where RH is the rainwater harvesting amount, A is the catchment area, P is the precipitation at the research site, and C is the runoff coefficient (the runoff coefficient of GBI is usually 0.15–0.4 (Nou and Charoenkit, 2020)). The calculated value is the rainwater collection potential of GBI, which can guide the size design of the water storage tank (dos Santos et al., 2019; Abdulla and Shareef, 2009).

Due to the simplification of the rainwater collection process, the empirical formula method is often used for the rough estimation of

[27] The Soil Conservation Service (SCS) Curve Number (CN) model; https://www.hec.usace.army.mil/confluence/hmsdocs/hmstrm/infiltration-and-runoff-volume/scs-curve-number-loss-model (retrieved on 25 November 2021)

Table 7
Methods review of rainwater collection by urban GBI.

Method	Spatial scale	GBI typology	Water-related Indicator	Empirical value	Reference
Experimental and Studies & Water Balance Equation (ES + WBE)	Building	Green roof (test bed)[a]	Rainwater collection Water saving rate	20 m^3 3%–5% (for urban plot of 520 m^2)	Charalambous et al., 2019
Experimental and Studies & Empirical Formulas (ES + EF)	City (921 km^2)	Green roof[a] (6.2 km^2)	Rainwater collection	1,503,728 m^3	dos Santos et al., 2019
Water Balance Equation & Model Simulation (WBE + MS: SWMM)	Community (6,000 people)	onstructed wetland[b] (1,002 m^2)	Irrigation water saving rate Total water saving rate	40% 27.2%	Li et al., 2017
Model Simulation (MS: Plugristost)	Building Neighborhood (981 people)	Green roof[a] Green roof[a] (684 m^2)	Rainwater collection Water self-sufficiency	7 m^3 21%–24%	Toboso-Chavero et al., 2019
	Technology park (1,786 people)	Green roof[a] (30,750 m^2)	Rainwater collection Water self-sufficiency	12,231 m^3 43%	Salvador et al., 2019
Experimental and Studies & Water Balance Equation & Model Simulation (ES + WBE + MS: MODFLOW)	Site	Rain garden[b] (30.24 m^2; 9.74 m^2)	Groundwater level increase	0.3 m	Li et al., 2019
Physical Method & Model Simulation (PM: SCS-CN + MS: SLAMM)	Residential zone (6.18 ha)	Permeable pavement[b] Grass swale[b]	Groundwater level increase rate	44% 72.6%	Zhang and Peralta, 2019

Note: [a] and [b] refer to the GBI with container-based rainwater collection means and soil-based rainwater collection means, respectively.

rainwater collection potential. To estimate the amount of collected rainwater more precisely, the water balance model is applicable, which is determined to the actual research boundary, mainly including precipitation, evapotranspiration, discharge runoff from GBI, irrigation water, soil matrix water, etc. Additionally, Toboso-Chavero et al. (2019) used the Plugristost model, which is also based on the water balance principle, to calculate the water tank size used for rainwater collection on the building roof, and it was found that a water storage tank of 7 m^3 installed on the rooftop was the appropriate size in their research.

Physical method (PM) is usually used to investigate the groundwater recharge of GBI. The water table fluctuation method is the most widely used method to estimate the groundwater recharge rate, which assumes that groundwater is recharged in an unconfined aquifer and results in an increase in the groundwater level (Tu and Traver, 2019). In addition, according to the water balance between surface runoff and groundwater recharge, the SCS-CN method calculates groundwater recharge considering rainfall, surface runoff, infiltration, and evaporation (Eaton, 2018). However, such calculated results through physical method are not the actual groundwater recharge, which cannot reflect the complete migration process of the surface water from the unsaturated soil area to the groundwater surface. There may be mismatches between the time and space scales of surface water and groundwater when simulating groundwater flows. Typically, model simulation is more efficient, as it does not require physical setups and fixed time spans. The commonly used models are MODFLOW[28], SWAT, SWMM, HYDRAUS, etc. Newcomer et al. (2014) utilized HYDRAUS to estimate and compare the groundwater recharge rate of infiltration ditches and irrigated lawns under historical (from 1954 to 2012), current (from 2011 to 2012), and future scenarios (from 2009 to 2100). The simulation showed that the annual recharge rate of the infiltration ditch to groundwater (3,410 mm/a) under the current and future scenarios was greater than that of the irrigated lawn (2,430 mm/a).

(iii) **Water purification**

Through leaf adsorption and soil infiltration, GBI can effectively reduce the concentration of pollutants in rainwater, and the pollution removal performance of GBI is significantly impacted by the rainfall characteristics and the inflow and outflow limits of GBI (Dhakal et al., 2017; Gong et al., 2019). However, GBI may introduce a new source of water pollution. Due to the nutrients within the manufactured media of GBI and fertilizers added during the production process, the concentration of the nutrient load was observed to be high in the effluent from GBI and has been a concern for water quality downstream, threatening the eutrophication risk for lakes and rivers (Kuoppamäki et al., 2016). Such effects on water quality from this implementation must be considered when generalizing the performance of GBI practices (Harper et al., 2015). From this review, we identified three main approaches used to evaluate the water quality from GBI: (a) field measurement (experimental studies (ES), observational studies (OS)), (b) statistical modelling (SM), and (c) model simulation (MS). The quantitative methods and results of the rainwater quality from GBI are shown in Table 8.

Field measurements refer to taking water samples from small GBI test devices or existing GBI sites and evaluating the water quality based on the pollutant concentrations measured in experiments. Leading water quality indicators include chemical oxygen demand (COD), nutrients (total nitrogen, total phosphorus, nitrate, nitrite, phosphate), sulfates, pH, suspended solids, chloride ions, fluorine ions, bromine ions, and metals (such as Ca, Mg, Na, K, Cu, Fe, Mn, Pb) (Vijayaraghavan et al., 2012; Wei et al., 2020; Roth et al., 2021; Denman et al., 2016). Gong et al. (2019) established a green roof test site on a building roof in Beijing, China, and simulated the real rainfall scenario to evaluate the runoff quality from green roofs. Their experimental results showed that extensive green roofs could significantly remove SS concentrations and reduce pollutant loads. However, the concentrations of COD, N, and P in the runoff discharged from the green roof were higher than those in the ordinary roof runoff. Likewise, according to Kuoppamäki et al. (2016), the nutrient concentrations in the runoff from green roofs were observed to be 5–10 times higher than those in the precipitation.

Field measurements are often carried out in laboratories or at the pilot scale but show limitations on a large scale (such as watersheds, cities, and regions). Due to the complex water flows of nonpoint source pollution, the deviation would happen between the evaluation results and actual situations of large-scale GBI if based on the small-scale results of GBI. Therefore, model simulation is typically used to evaluate the

[28] https://www.usgs.gov/mission-areas/water-resources/science/modflow-and-related-programs (retrieved on 25 November 2021)

Table 8
Methods review of water quality from urban GBI.

Method	Spatial scale	GBI typology	Water-related Indicator	Empirical value	Reference
Experimental Studies & Statistical Modelling (ES + SM)	Building	Green roof (test bed, 0.2 m^2)	Pollutant removal rate	24% (TN); 27% (TP) (Biochar A)	Kuoppamäki et al., 2016
	Roadway (54.8 m^2)	Bioretention cell	Pollutant removal rate Pollutant increase rate	17.46% (TP) 196% (TN); 317% (TSS)	Lucke and Nichols, 2015
	Parking lot	Bioretention cell	Pollutant removal rate Pollutant increase rate	48%–62% (TKN); 42%–56% (Organic N); 78%–87% (TAN); 32%–35%(TN); 12%–19% (TP); 79%–89% (TSS) 25%–103% (NO_x)	Brown and Hunt, 2012
	Parking lot	Bioretention cell (35 m^2)	Pollutant removal rate	>99% (Sediment; TN; TP)	DeBusk and Wynn, 2011
Experimental Studies & Water Balance Equation & Statistical Modelling (ES + WBE + SM)	Parking lot (881.6 m^2)	Permeable pavement (209 m^2)	Pollutant removal rate	12%–76% (TSS; BOD5; Escherichia coli)	Mahmoud et al., 2020
Observational Studies & Water Balance Equation & Model Simulation (OS + WBE + MS: RECARGA)	City	Green roof (1000 m^2), bioretention cell (50 m^2), detention basin	Pollutant removal rate	63%–88%	Kristvik et al., 2019
Model Simulation (MS: MIKE)	Region (28.1 km^2)	Bioretention cell, permeable pavement, green roof (with total area of 1.04 km^2)	Increased pollutant removal rate compared with the basic scenario	19.2%–68.7% (TSS); 19.2%–67.8% (COD); 18.7%–60.9% (TN); 19.9%–68.8% (TP)	Li et al., 2018
Model Simulation (MS: HEC-RAS and QUAL2K)	Basin	Constructed wetland	Pollutant removal rate	13.6%–25.6% (TN); 50.0%–50.9% (TP)	Xiao et al., 2020
Spatial Analysis & Experimental Studies & Statistical Modelling (SA + ES + SM)	Basin	Constructed wetland	Pollutant removal rate	65%–86% (TSS)	Yang et al., 2014

water purification effect of GBI on a large scale. Commonly used models are InVEST[29], HEC-RAS, QUAL2K[30], i-Tree, RECARGA[31], etc., of which i-Tree and RECARGA bring high accuracy and are more suitable for simulating the water purification effect of local-scale GBI. Kristvik et al. (2019) used the RECARGA model to examine the rainwater purification performance of biological detention tanks. The long-term simulation results showed that the biological detention tank could reduce rainwater runoff by 54%–85% and filter 63%–88% of rainwater pollutants. InVEST, HEC-RAS, and QUAL2K are more often used to simulate the water purification effect of GBI in the subregional and regional scales. Xiao et al. (2020) used HEC-RAS and QUAL2K to predict and evaluate the nutrient removal rate of the Edmonton wetland in Canada. The research showed that the removal efficiency of wetlands for total nitrogen (TN) was 25.6% and 13.6%, respectively, by these two models, and the removal efficiency of wetlands for total phosphorus (TP) was 50.0% and 50.9%, respectively.

5. Life cycle assessment to quantify the trade-offs of GBI

This section aims to outline the relevant studies to capture GBI's trade-offs based on the life cycle thinking, given that a silo lens of FWE-related benefits of GBI cannot reflect the comprehensive implications of GBI on FWE nexus. Regarding previous trade-offs studies, two streams are shown, that is, the trade-offs between life cycle environmental impacts and operational benefits of GBI, and the food-water-energy-carbon nexus trade-offs of GBI in the upstream production and supply chains. The corresponding studies and findings are summarized in the following contents and Tables 9–10.

5.1. Trade-offs between life cycle environmental impacts and operational benefits

Urban GBI positively affects the FWE systems through local food provision, energy supply and savings, rainwater harvesting and purification, among others. Yet the FWE-related benefits are presented with GBIs' expansion at the cost of elevated greenhouse gas emissions, resource and energy consumption, and other adverse environmental impacts throughout the entire lifespan. A life cycle perspective is hence imperative to achieve the holistic design, implementation, and management of GBIs, and life cycle assessment (LCA) has been increasingly applied to evaluate the cradle-to-grave performance of various GBI technologies associated with materials, construction, maintenance, decommission, and disposal (Spatari et al., 2011; Shafique et al., 2020).

The LCA studies exploring GBIs' environmental performance currently show two streams. One is the specific focus on the environmental impacts of GBI (Andrew and Vesely, 2008; Manso et al., 2018; Pushkar, 2019), and the other is the detailed consideration of the life cycle impacts and operational benefits (De Sousa et al., 2012; Wang et al., 2013; Moore and Hunt, 2013; Xu et al., 2021). The former tends to apply the LCA method to evaluate the environmental performance of GBIs, considering all life cycles including the stages of material production, transportation, construction, operation, and end of life. Such studies generally aim to identify which materials and processes of the green and blue systems have greater environmental burdens and to determine how these impacts can be minimized (Manso et al., 2018). These LCA studies are helpful for architects, ecologists, and engineers to find new solutions to alleviate the life cycle burdens of urban GBIs by applying more environmentally friendly materials and technologies (Pushkar, 2019).

To date, the above evaluation of specific life cycle impacts of GBI draws the main attention. However, it was revealed that such a single focus on environmental impacts would risk underestimating the intangible benefits within the stage of operation and maintenance (Chàfer et al., 2021). For the system-wide assessment of urban GBI strategy, attempts have been made to analyse the trade-offs of GBI. These studies have considered the environmental impacts in the whole life cycle and the FWE-related benefits in the operation stage, helping designers and technology developers to understand the potential as well as the environmental concerns associated with GBI and to evaluate the long-term environmental sustainability of this system (Pan and Chu, 2016). As shown in Table 9, these LCA research on the trade-offs evaluation of GBI can be summarized as the following categories: (a) individual application of GBI, (b) comparison of multiple GBIs, (c) comparison of GBIs with grey infrastructure systems, and (d) integration of GBIs into the

[29] https://naturalcapitalproject.stanford.edu/software/invest (retrieved on 25 November 2021)
[30] https://www.qual2k.com/
[31] https://dnr.wisconsin.gov/topic/Stormwater/standards/recarga.html

Table 9
Trade-offs analysis of urban GBI based on the LCA method.

Research category	GBI typology	Boundary	Scale	Environmental impacts	Benefits provided by GBI	Findings	Reference
a	Vertical greenery system	Materials, transportation, use and end of life	Building	Global warming, acidification, eutrophication, ozone layer depletion, abiotic depletion elements, abiotic depletion fossil, freshwater aquatic ecotoxicity, human toxicity, marine aquatic ecotoxicity, photochemistry ozone creation, terrestrial, and ecotoxicity	Energy saving due to the cooling effect of vegetation	The initial energy investment of vertical greenery could be paid back within 40 years, and the carbon emission reductions from energy generation were able to offset the costs of global warming over the 50-year life span	Pan and Chu, 2016
a	Vertical greenery system	Manufacturing, construction, operation, maintenance and end of life	Cubicles experimental set-up site	Human health, ecosystem quality, resource scarcity, and global warming	Energy saving	The energy saving for heating and cooling can reduce environmental burdens by 1% annually, and the reduction in summer can be up to almost 50%	Chàfer et al., 2021
a	Green roof	Materials, transportation, construction, maintenance, disposal and end of the life	1,115m^2 roof on a retail store	Human health, ecosystem quality, climate change, and resources	Energy saving, runoff control	The environmental impacts can be reduced by the benefits of energy saving and runoff reduction	Kosareo and Ries, 2007
a	Green roof	Extraction and refinement of raw materials and consumption of natural resources	Building	Carbon dioxide emission	Carbon sequestration, carbon emission reduction by energy saving	The life cycle carbon emissions could be offset by carbon sequestration and carbon reduction by energy saving in 5.8 to 15.9 years	Kuronuma et al., 2018
a	Green roof	Material production, transportation, building operation and building maintenance	Building	Global warming, acidification, eutrophication, ozone layer depletion, abiotic depletion, freshwater aquatic ecotoxicity, human toxicity, marine aquatic ecotoxicity, photochemistry oxidation, and terrestrial ecotoxicity	Energy saving, water saving	The life cycle environmental impacts can be reduced by 1%-5.3% due to energy saving, and the water saving benefit could further reduce the life cycle impacts by 0.2%–2.0%	Saiz et al., 2006
			City			The life cycle environmental impacts would be reduced by even five times more	
a	PV-green roof	Material manufacturing, transportation, use/maintenance, and disposal	Building	Noncarcinogens, respiratory inorganics, global warming and non-renewable energy, carcinogens, ionizing radiation, ozone layer depletion, respiratory organics, aquatic ecotoxicity, terrestrial ecotoxicity, terrestrial acidification/nutrification, land occupation, aquatic acidification, aquatic eutrophication, and mineral extraction	Energy generation	The significant energy generation potential of PV-green roofs in the use phase could compensate for their additional environmental impacts	Lamnatou and Chemisana, 2014
a	Bio-infiltration rain garden	Implementation, operation, and decommissioning	Site	Global warming potential, acidification, cancer, non-cancer, respiratory effects, eutrophication, ozone depletion, and ecotoxicity	Carbon sequestration, air pollutant removal, runoff control, rainwater pollutant removal, and energy savings due to reduced volume at a wastewater treatment plant	The positive operation effects could avoid more than 11 times the adverse construction impacts on global warming potential, eutrophication potential, and eco-toxicity	Flynn and Traver, 2013

(*continued on next page*)

Table 9 (*continued*)

Research category	GBI typology	Boundary	Scale	Environmental impacts	Benefits provided by GBI	Findings	Reference
b	Green roof, rain garden, bioretention basin, vegetated swale, and stormwater pond	Material production, construction, operation, maintenance and end of life	Building/ site	Carbon emission	Carbon sequestration	Due to the highest carbon sequestration potential, rain garden could offset total carbon footprint in its life cycle and had the lowest net carbon footprint. Whereas stormwater pond had the maximum life cycle carbon footprint with lowest carbon sequestration potential	Kavehei et al., 2018
b	Green roof, greenway, and grove	Extraction, transportation, construction, use, maintenance, and end of life	Neighborhood	Global warming, acidification, eutrophication, respiratory inorganics, water use, abiotic depletion, and Chinese resource depletion potential	Energy saving	Groves showed the best overall environmental performance than greenways and green roofs within system boundary, due to the significant energy saving potential of groves than those two	Wang et al., 2020
b	Green roof, permeable pave, bioretention, constructed wetland, Level spreader-vegetated filter strip, pond, rainwater harvesting system	Materials, transportation, construction and maintenance	Site	Carbon emission	Carbon sequestration	Constructed wetland were predicted to offset the life cycle carbon emissions, with the lowest net carbon footprint over a 30-year period, followed by bioretention, level spreader-vegetated filter strip, pond, permeable pave, green roof, and rainwater harvesting system	Moore and Hunt, 2013
b	Green façade and living wall systems	Materials, transportation and waste	Building	Global warming, acidification, eutrophication, ozone layer depletion, abiotic depletion, freshwater aquatic ecotoxicity, human toxicity, marine aquatic ecotoxicity, photochemistry oxidation, and terrestrial ecotoxicity	Energy saving	Vertical greenery shows positive improvement of environmental performance with lower impacts, due to a reduction of energy savings during the life span of a greened building	Ottelé et al., 2011
b, c, d	Green alternatives (bioretention basin, green roof, and permeable pavement); Existing combined sewer system, and separate sewer system; Integration alternatives that combine one green alternative with the separate sewer system	Material extraction and production, material and waste transportation, installation, and maintenance.	Watershed	Climate change, freshwater eutrophication, marine eutrophication, freshwater ecotoxicity, and fossil fuel depletion	Rainwater pollutant removal	Bioretention basin results in the least climate change and economic costs in the construction phase for water pollutant removal, and separate sewer system consumes the least energy for removing pollutants	Wang et al., 2013
c	Combination of porous pavement, street-end bioretention bump-out facility, curbside infiltration planter, backyard rain garden, and subgrade cistern; Grey combined sewer overflows	Construction, operation, and maintenance	Watershed	Greenhouse gas emissions	Carbon sequestration, carbon emission reduction due to the building energy saving by shading and wind blocking of vegetation	Compared with gray infrastructure, the combination of decentralized GBI had superior environmental performance, with 75%–95% lower GHG emissions than gray infrastructure scheme	De Sousa et al., 2012

(*continued on next page*)

Table 9 (*continued*)

Research category	GBI typology	Boundary	Scale	Environmental impacts	Benefits provided by GBI	Findings	Reference
c	Rain garden; Existing combined sewer and wastewater treatment systems	Construction, operation, and decommissioning	Watershed	Acidification, ecotoxicity, eutrophication, global warming, ozone depletion, photochemical oxidation, carcinogenics, noncarcinogenics, and respiratory effects	Carbon sequestration, water storage and treatment	Rain gardens were revealed to be a favorable option by decreasing 42% of the financial cost and 62–98% of the life cycle impacts, compared to the grey infrastructure alternative. Rain gardens had dramatic decreased impacts in eutrophication and global warming by intercepting nutrient pollution before it can reach the wastewater and by reducing the use of electricity for wastewater treatment	Vineyard et al., 2015
b, c	Best management practices (BMPs: vegetated swale, rain garden, porous pavement); Traditional structures (porous detention basin, sand filter detention basin)	Construction, operation and maintenance	City	Climate change, terrestrial acidification, freshwater eutrophication, marine eutrophication, and terrestrial ecotoxicity	Runoff control	The implementation of green BMPs did effectively reduce LCA impacts compared with traditional management strategies, in which porous pavements generally resulted in slightly higher impacts compared with rain gardens and vegetated swales	Hengen et al., 2016
b, c	bioswale, grass swale, detention basin, retention basin, culvert, storm sewer, and pipe underdrain	Construction, maintenance, and end-of-life	Roadway	Ozone depletion, climate change, smog, acidification, eutrophication, carcinogens, noncarcinogens, respiratory effects, ecotoxicity, fossil fuel depletion, and cumulative energy demand	Rainwater pollutant removal	The local aquatic benefits of grass swales and bioswales offset global environmental impacts for eutrophication, carcinogenics, noncarcinogenics, and ecotoxicity	Byrne et al., 2017
b, c, d	Hybrid system that combines low impact development (LID: bioretention areas, rooftop rainwater harvesting, and xeriscaping) technologies with conventional centralized water systems.	Construction and maintenance	Apartment zone	Global warming, ozone depletion, smog formation, acidification, eutrophication, carcinogens, noncarcinogens, respiratory effects, ecotoxicity, and fossil fuel depletion	Rainwater harvesting	Incorporating LID in residential zones can help collect rainwater and reduce potable water use with an average of 25%–50% by treating rainwater to potable quality	Jeong et al., 2016
c, d	Hybrid system that combines green infrastructure system (bioretention, permeable pavement, green roof, detention cell, adjusted pipeline) and gray system (original pipeline)	Materials, transportation, construction, and operation	Catchment area	Global warming, ozone formation, noncarcinogens, carcinogens, ionizing radiation, ozone layer depletion, particulates formation, terrestrial acidification, aquatic eutrophication, freshwater ecotoxicity, marine eutrophication, land occupation, water depletion, metal depletion, and fossil depletion	Runoff control and rainwater pollutant removal	Hybrid system generated higher environmental impacts and economic costs than grey system in the construction stage. However, the economic benefits of coupled system are shown in comprehensive water benefits during the operational stage, which can make the payback time of total economic cost within 4 years	Xu et al., 2021

Note: * a individual application of GBI; b comparison of multiple GBIs; c comparison of GBIs with grey infrastructure systems; d integration of GBIs into the existing grey infrastructure systems.

existing grey infrastructure systems. Among these studies, most simply considered certain types of GBI, while coupled "grey and green–blue" infrastructure systems take the least focus.

The evaluation of trade-offs of GBI frequently focuses on the benefits of rainwater collection, runoff reduction, removal of rainwater pollutants, energy savings for wastewater treatment, carbon sequestration, building energy savings due to the influence of vegetation by shading and wind blocking, carbon emission reduction by energy savings, and

Table 10
Food-water-energy-carbon nexus quantification of urban GBI.

GBI-FWE	Nexus	GBI typology	Method	Findings	Reference
GBI-Food	Food-Carbon	Urban agriculture	MFA	If the Seoul metropolis implemented urban agriculture in a 51.15 km^2 area, it would be possible to reduce CO_2 emissions by 11.67 million kg annually	Lee et al., 2015
		Rooftop farm	MFA	If 121,599 ton of vegetables are produced annually in HDB estates in green roofs in Singapore, there will be a reduction of 9,052 ton of CO_2 emissions per year	Astee and Kishnani, 2010
		Rooftop farm	LCA	The avoided CO_2 emissions of rooftop tomato cultivation for each inhabitant per year is 18.1 kg	Toboso-Chavero et al., 2019
		Rooftop farm	LCA	150,000 kg of tomatoes in 1 ha rooftop gardens in Barcelona could represent a saving of 66.1 tons CO_2	Sanyé-Mengual et al., 2013
		Rooftop farm	LCA	2,000 ton of tomatoes per year produced in rooftop gardens in the Zona Franca Park could avoid approximately 850 ton of CO_2	Sanyé-Mengual et al., 2015
		Rooftop farm	LCA	29 ton of CO_2 per year could be avoided if lettuce and tomato are cultivated almost 14,000 kg/year in the rooftop garden in Rio de Janeiro, Brazil	Salvador et al., 2019
		Community farm	LCA	Converting 26 ha of vacant land to community farming would reduce GHG emissions by 881 ton per year	Kulak et al., 2013
	Food-Energy	Rooftop farm	LCA	150,000 kg of tomatoes in 1 ha rooftop gardens in Barcelona could represent a saving of 2,070 MJ of energy consumed	Sanyé-Mengual et al., 2013
		Rooftop farm	LCA	2,000 ton of tomatoes per year produced in rooftop gardens in the Zona Franca Park could avoid approximately 23.1 TJ of energy	Sanyé-Mengual et al., 2015
	Food-Water	Urban agriculture	LCA	Local lettuce cultivation could reduce 50% of water footprint	Yang and Campbell, 2017
		Urban agriculture	LCA	Shifting 1 ha of cropping land from vegetables to cereals could reduce local blue water consumption by 7,216 m^3 per year	Huang et al., 2014
GBI-Energy	Energy-Carbon	Rooftop garden	LCA	Almost 767 ton of CO_2 per year can be avoided by 3,009,000 kWh/year of PV energy generation in the rooftop garden	Salvador et al., 2019
		Green roof	MFA	The avoided upstream CO_2 emissions due to energy saving were estimated to be 7.4×10^4 ton and 1.3×10^5 ton for extensive green roofs and intensive green roofs, respectively	Peng and Jim, 2015
		Green roof	MFA	In the Turin context, using insulated green roofs, there was an annual reduction of GHG emissions of 193 ton and 14 ton of CO_2 per MWh for energy of heating up and cooling	Todeschi et al., 2020
		Green wall	MFA	697 kg of CO_2 can be avoided due to approximately 985.6 kWh of electricity saving	Campos-Osorio et al., 2020
		Green wall	MFA	The double-skin green façade has the potential to reduce 2.2×10^9 kg of carbon dioxide emission in a year	Wong and Baldwin, 2016
		Green wall	MFA	The intensity of carbon emission reduction in winter is 2.2–4.2 kg per week	Cameron et al., 2015
GBI-Water	Water-Carbon	Rooftop farm	LCA	Nearly 9 ton of CO_2 can be avoided per year by harvesting rainwater in the rooftop gardens	Salvador et al., 2019
		Rooftop farm	LCA	The application of rainwater harvesting in rooftop gardens could potentially avoid 0.45 kg CO_2 per year for each inhabitant	Toboso-Chavero et al., 2019
		Urban agriculture	MFA and DAYCENT model	A 33% reduction in life cycle system-wide GHG emissions can be achieved by wastewater treatment and reuse	Miller-Robbie et al., 2017
		Green roof, bioretention basin, permeable pavement, rain garden, and vegetated swale	MFA	GHG emissions via urban drainage systems and water supply systems can be reduced by 10,677.3 and 6,837.1 ton per year respectively in the study area	Liu et al., 2020
	Water-Energy	Permeable pavement	MFA	4.1% of annual energy cost for water treatment can be saved	Lee and Kim, 2016
		Green roof	MFA	3.46 US$/$m^3$ of annual energy cost for rainwater management can be saved in Berlin	Zhang et al., 2015

Note: MFA is short for Material Flow Analysis.

removal of atmospheric pollutants. The considered environmental impacts of GBI over the entire life history include common impact categories, such as global warming, resource and energy consumption, eutrophication potential, ecotoxicity, and land occupation. In addition, the carbon footprint, based on the definition by Wiedmann and Minx (2008), is also presented as a single indicator of global warming potential or climate change impact.

The estimates of life cycle impacts released by GBI vary significantly and depends on the type and lifespan of GBI as well as the study area characteristics. Some of the studies struggle to investigate the external impacts related to the stage of construction, maintenance, and decommissioning of GBI practices, excluding their upstream impacts associated with raw material extraction and production (De Sousa et al., 2012; Vineyard et al., 2015; Hengen et al., 2016; Jeong et al., 2016; Byrne et al., 2017). However, during the whole life cycle of the urban GBI, most of the environmental impacts of GBI are incurred in the manufacturing phase and the construction phase because of a large amount of material and resource consumption (Pushkar, 2019; Oquendo-Di Cosola et al., 2020). As a result, a broader scope of research is necessary to promote the assessment effectiveness of GBI. It is also pointed out that transport emissions are a major contributor to the carbon footprints of GBI, since the materials for GBI manufacturing need to be transported to specfic sites from other places. Thus, the localization of material resources should be encouraged to decrease these effects (Kavehei et al., 2018). Regarding studies that calculated the carbon footprints of GBI, some of them were limited to CO_2 emissions (Moore and Hunt, 2013; Kuronuma et al., 2018). However, GBIs are likely to emit other greenhouse gases (i.e., nitrous oxide and methane), and further work needs to expand these estimates to global warming potential to avoid the one-sided impact evaluation on climate change.

Although life cycle assessment is an established technique for the analysis of the environmental impacts of programs, and practitioners along with academics have paid increasing attention in recent years to the trade-offs of GBI with respect to their so-called operational benefits and life cycle environmental impacts, current studies are part of attempts to develop and test an LCA methodology specific to GBI practices, which are in their infancy. To be concrete, the particular focus on carbon sequestration, stormwater runoff quantity and quality, and energy savings comprise the main proportions of the trade-offs studies of GBI (Liu et al., 2016; O'Sullivan et al., 2015; Spatari et al., 2011; Vineyard et al., 2015). Benefits beyond the aforementioned include biodiversity, recreation opportunities, community aesthetics, human health, and employment opportunities, which are deemed outside the scope of current studies but need to be explored. Large upfront investments and social impacts (such as noise pollution towards dwellers during construction) should also be considered in future cases (Flynn and Traver, 2013).

In addition, there are still controversies regarding the different results within various temporal and spatial scales, and the assessments were mainly conducted at the site scale. Thus, the tendency needs to be targeted at the upscaling research (i.e., cities and regions) and applicability investigation of the impact scaling techniques through GBI case studies in different sizes and scales. More frequently, the environmental trade-offs varying among different types of GBIs were not clear, and the analysis is limited by the availability of requisite datasets. A toolbox for embracing data-sharing mechanisms and quantitative models would break such obstacles and promote the sustainability assessment of GBIs in relation to their environmental benefits and costs.

5.2. Food-water-energy-carbon nexus trade-offs

The relation between climate change and FWE in cities has become increasingly relevant in the literature (Benites-Lazaro et al., 2022). GBI can provide FWE-related benefits and reduce the demand for FWE supply in cities. Seen from the complex production systems and trade supply chains, the direct effects of GBI on FWE within urban boundaries could further avoid the trans-boundary environmental footprints embodied in upstream supply chains, such as energy consumption, water consumption, and carbon emissions (Ramaswami et al., 2017). Based on these trans-boundary interactions, the food-water-energy-carbon (FWEC) nexus associated with GBI is clarified as the GBI-FWEC linkage. Among the quantitative research (Table 10), the food sector is the most studied since the localization of food production is advocated as a climate-resilient pathway (Toboso-Chavero et al., 2019; Yang and Campbell, 2017; Sanyé-Mengual et al., 2015), and carbon emissions are the most widely concerning issue in the context of increasing global warming (Salvador et al., 2019; Miller-Robbie et al., 2017).

Notably, local food production and its consequently decreasing carbon emissions have received most of the attention. The main reason is that urban food production from GBI can reduce food import demand and food mileage, thereby avoiding carbon emissions embodied in the upstream food supply chain, which is expected to yield positive effects in relation to climate change (Bellezoni et al., 2021). However, it is noted that despite the indirect benefits beyond city boundaries, there may be contradictory effects within cities. If more local food production is not based on rainwater harvesting/reuse, the demand for water could increase, causing negative impacts on this system. Likewise, it could have indirect negative effects on energy use and carbon emissions. In addition, to the best of our knowledge, comprehensive energy studies have focused on carbon emissions, which are avoided by energy saving and energy generation induced by GBI. Green roofs are a particularly popular adaptation by which the mitigation of carbon emissions can be assessed because they can reduce building temperatures and thus reduce the energy consumed by air conditioning and heating (Liu et al., 2020). Regarding water, the avoided carbon emissions due to the rainwater management benefits of GBI receive primary focus, in the aspects of decreasing water supply through rainwater collection, and decreasing wastewater drainage and treatment through runoff control and pollutant removal.

It was revealed that the existing studies tended to quantify one of these linkages in isolation (i.e., food-carbon, food-energy, food-water, energy-carbon, water-carbon, water-energy), while few studies shed lights on the trans-boundary or cross-sectoral effects of GBI on energy, water, and carbon footprints from a nexus lens. Two representatives of the research between FWE sectors and carbon emissions are from Toboso-Chavero et al. (2019) and Salvador et al. (2019). Based on different combinations of food and energy production and rainwater harvesting implementations on rooftops at the neighborhood scale in Barcelona, Toboso-Chavero et al. estimated the degree of self-sufficiency of food, water, and energy and the equivalent amount of avoided carbon dioxide emissions and evaluated the corresponding environmental implications of different rooftop strategies. Salvador et al. established a procedure to determine the self-sufficiency potential of rooftop gardens in a Brazilian technology park through food production, renewable energy generation, and rainwater harvesting. Further, they developed the Nexus Emission Index indicator to estimate the avoided CO_2 emissions by not using conventional systems (i.e., imported food and energy and water networks).

Despite some progress, given that the internal multi-linkages between GBI and the FWEC nexus remain unknown partially but as critical issues (e.g., embodied water consumption during energy generation, among others), we see a need for a systemic quantification of the linkages between GBI and FWEC nexus to track their dynamic flows over space and time. A nexus approach would function for this by examining the interactions among sectors and uncovering the trade-offs across scales (Liu et al., 2018). For instance, regarding the issue of food security, the silo lens shapes our top priority in thinking of the hindrance during food production or supply. Conversely, the nexus approach with cross-sectoral and trans-boundary perspectives leads to our deep consideration of possible increased carbon tax pressure for producers, water shortages for fresh food preservation, and energy risks for food

logistics outside cities. With the aim of SDGs and their interconnections, the nexus approach emerges as a potential strategy to manage urban nexus challenges and guide pathways to achieve these goals (Ringler et al., 2013; Rasul and Sharma, 2016), including SDG2 (zero hunger), SDG6 (clean water), SDG7 (sustainable energy), and SDG13 (on climate action). In this review, we highlight the critical role of the FWEC nexus approach and a nexus framework for clarifying complex relationships between GBI and FWEC across sectors and city boundaries and provide a foundation for further analysis. We believe the FWEC nexus approach would be helpful for stakeholders and administrators in planning and governing the urban resilience of FWE systems and sustainability in the face of future uncertainties at the scale of metropolitan regions and cities, such as production and supply risks (de Oliveira et al., 2022).

6. Conclusions and Discussion

Urban GBI has gained increasing popularity for urban resilience and sustainability through adaptive and flexible implementations in the context of current unsustainable paths of urbanization. In particular, research efforts have been made to evaluate the fundamentality of GBI in improving FWE issues since the FWE security nexus topic was released at the conference. This study identifies the detailed connections between urban GBI and FWE nexus and provides a method review for the linkages between GBI and FWE nexus, including FWE-related benefits and trade-offs of environmental benefits and costs together with FWEC nexus, which helps to improve our understanding of their intrinsic dynamics.

The review of past research shows that most of the studies focus on the FWE-related benefits or (and) life cycle impacts of GBI from a silo perspective, while less attention has been given to the avoided trans-boundary environmental footprints by GBI's benefits. In myriad studies on the benefit measurement of different types of GBI, it was found that the outcomes are not reported consistently across these studies. This can be attributed to the differences in quantified methods (e.g., agricultural logbooks, statistical data, experimental and observational studies, model simulation, statistical modelling, empirical formulas, water balance equations), GBI adopted (e.g., green roofs, green walls, community gardens, constructed wetlands, street trees, green space, urban forest), and research scope (e.g., site, building, neighborhood, district, city, country, world). Regarding the trade-offs evaluation of GBI, LCA research takes a mature whole-of-system approach from "cradle-to-grave" to allow quantification, involving a wide range of environmental impacts and operational benefits. However, as for the cross-sectoral and trans-boundary linkages between GBI and FWE nexus, the indirect energy-water-carbon footprints related to GBI are not typically accounted for in full. Existing studies show the tendency to the embodied impacts singly (e.g., food-carbon, food-energy, food-water, energy-carbon, water-carbon, water-energy) rather than revealing the underlying complex interactions between food-water-energy-carbon in urban GBI systems.

Current quantitative methods have paved the way to better understand the interlinkages between GBI and FWE nexus as well as quantify the trade-offs of GBI based on life cycle thinking and the FWE nexus perspective. However, these methods are relatively scattered and lack integrated quantitative guidance. The main knowledge gaps are related to the systematic accounting on FWE-related impacts, as well as understanding the LCA-based environmental effects and both the resultant trans-boundary and cross-sectoral FWE nexus impacts from urban GBI. The lack of sufficient data also contributed to those gaps. For instance, the food-related monitoring data in the operational stage are probably more readily available than most other energy- and water-related impacts. The conventionally agreed factors of life cycle performance of GBI are frequently applied instead of the localized parameters, and researchers may fail to visualize the trans-boundary interactions from local to region and globe, which are both limited by the data availability. Therefore, establishing a credible local data system is an important basis for exploring the interlinkages between GBI and FWE nexus. Furthermore, the static LCA limits researchers from undertaking dynamic simulations of energy-water-carbon flows associated with GBI. In view of the diversity and multifunctionality of urban GBI typologies and the multielement, multisectoral characteristics of urban FWE nexus, quantification research on the linkages between GBI and FWE nexus should be carried out dynamically (Shannak et al., 2018). For instance, Bixler et al. (2019) integrated a system dynamic model (validated through historical data) into an LCA framework to allow the future predictions of trade-offs of GBI under different geographical locations, land uses, sizes, and climate change scenarios, which is proven as a pioneering effort.

Consequently, we call for a holistic methodological framework that dynamically simulates the interlinkages between urban GBI and FWE nexus. We also suggest that future research explore the possible methods of downscaling and upscaling to apply the research findings to more widely specific scales and facilitate the systematic understanding of urban GBI and FWE nexus. The expertise in embracing the assessment practices of GBI on FWE nexus at the city scale makes it promising to guide policy-makers with insights into FWE-oriented urban sustainable planning and governance starting from GBI.

CRediT authorship contribution statement

Fanxin Meng: Conceptualization, Supervision, Writing-original draft, Funding acquisition. **Qiuling Yuan:** Methodology, Investigation, Data curation, Visualization, Writing-original draft. **Rodrigo A. Bellezoni:** Conceptualization, Methodology, Writing-Review, Editing. **Jose A. Puppim de Oliveira:** Writing-Review, Editing, Funding acquisition. **Silvio Cristiano:** Writing-Review, Editing. **Aamir Mehmood Shah:** Methodology, Data curation. **Gengyuan Liu:** Writing-Review, Editing. **Zhifeng Yang:** Conceptualization, Supervision. **Karen C. Seto:** Conceptualization, Investigation, Supervision, Funding acquisition.

Declaration of Competing Interest

The authors declare that they have no known competing financial interests or personal relationships that could have appeared to influence the work reported in this paper.

Data Availability

No data was used for the research described in the article.

Acknowledgements

We would like to appreciate support from the National Natural Science Foundation of China (No. 72174028) and the Belmont Forum (grant number NEXUS2016: 152); the JPI Urban Europe (grant number 11221480); the NSF, USA (award number 1829224); the FAPESP Foundation, Brazil (grant numbers 2017/50425-9 and 2018/20057-0); Coordination for the Improvement of Higher Education Personnel (CAPES) grant number 88881.310380/2018-01; and National Council for Scientific and Technological Development (CNPq) grant number 442472/2020. This paper is part of the results of the JPI Urban Europe and Belmont Forum project IFWEN (Understanding Innovative Initiatives for Governing Food, Water and Energy Nexus in Cities, https://jpi-urbaneurope.eu/project/ifwen/)

Supporting Information

Quantification of food, water, and energy topics related to urban GBI (Table S1).

Supplementary materials

Supplementary material associated with this article can be found, in the online version, at doi:10.1016/j.resconrec.2022.106658.

References

Abdulla, F.A., Al-Shareef, A.W., 2009. Roof rainwater harvesting systems for household water supply in Jordan. Desalination 243 (1–3), 195–207. https://doi.org/10.1016/j.desal.2008.05.013.

Akbari, H., Kurn, D.M., Bretz, S.E., Hanford, J.W., 1997. Peak power and cooling energy savings of shade trees. Energy Build. 25 (2), 139–148. https://doi.org/10.1016/s0378-7788(96)01003-1.

Alexandri, E., Jones, P., 2008. Temperature decreases in an urban canyon due to green walls and green roofs in diverse climates. Build. Environ. 43 (4), 480–493. https://doi.org/10.1016/j.buildenv.2006.10.055.

Algert, S.J., Baameur, A., Renvall, M.J., 2014. Vegetable output and cost savings of community gardens in San Jose, California. J. Acad. Nutr. Diet. 114 (7), 1072–1076. https://doi.org/10.1016/j.jand.2014.02.030.

Alihan, J.C., Flores, P.E., Geronimo, F.K., Kim, L., 2018. Evaluation of a small HSSF constructed wetland in treating parking lot stormwater runoff using SWMM. Desalination Water Treat 101, 123–129. https://doi.org/10.5004/dwt.2018.21823.

Andrew, R.M., Vesely, E.T., 2008. Life-cycle energy and CO_2 analysis of stormwater treatment devices. Water Sci. Technol. 58 (5), 985–993. https://doi.org/10.2166/wst.2008.455.

Arghavani, S., Malakooti, H., Bidokhti, A.A.A.A., 2020. Numerical assessment of the urban green space scenarios on urban heat island and thermal comfort level in Tehran Metropolis. J. Clean. Prod. 261, 121183 https://doi.org/10.1016/j.jclepro.2020.121183.

Astee, L.Y., Kishnani, N.T., 2010. Building integrated agriculture: Utilising rooftops for sustainable food crop cultivation in Singapore. J. Green Build. 5 (2), 105–113. https://doi.org/10.3992/jgb.5.2.105.

Avellán, T., Gremillion, P., 2019. Constructed wetlands for resource recovery in developing countries. Renew. Sustain. Energy Rev. 99, 42–57. https://doi.org/10.1016/j.rser.2018.09.024.

Baumann, T., Nussbaumer, H., Klenk, M., Dreisiebner, A., Carigiet, F., Baumgartner, F., 2019. Photovoltaic systems with vertically mounted bifacial PV modules in combination with green roofs. Sol. Energy 190, 139–146. https://doi.org/10.1016/j.solener.2019.08.014.

Bautista, D., Peña-Guzmán, C., 2019. Simulating the hydrological impact of Green roof use and an increase in Green areas in an urban catchment with i-tree: a case study with the town of Fontibón in Bogotá, Colombia. Resources 8 (2), 68. https://doi.org/10.3390/resources8020068.

Bellezoni, R.A., Meng, F., He, P., Seto, K.C., 2021. Understanding and conceptualizing how urban green and blue infrastructure affects the food, water, and energy nexus: a synthesis of the literature. J. Clean. Prod. 289, 125825 https://doi.org/10.1016/j.jclepro.2021.125825.

Benites-Lazaro, L.L., Giatti, L.L., Macedo, L.S.V, Puppim de Oliveira, J.A., 2022. Water-Energy-Food Nexus and Climate Change in Cities. Springer Nature.

Berardi, U., 2016. The outdoor microclimate benefits and energy saving resulting from green roofs retrofits. Energy Build. 121, 217–229. https://doi.org/10.1016/j.enbuild.2016.03.021.

Berry, R., Livesley, S.J., Aye, L., 2013. Tree canopy shade impacts on solar irradiance received by building walls and their surface temperature. Build. Environ. 69, 91–100. https://doi.org/10.1016/j.buildenv.2013.07.009.

Biggs, E.M., Bruce, E., Boruff, B., Duncan, J.M., Horsley, J., Pauli, N., McNeil, K., Neef, A., Van Ogtrop, F., Curnow, J., Haworth, B., Duce, S., Imanari, Y., 2015. Sustainable development and the water–energy–food nexus: a perspective on livelihoods. Environ. Sci. Polic. 54, 389–397. https://doi.org/10.1016/j.envsci.2015.08.002.

Bixler, T.S., Houle, J., Ballestero, T., Mo, W., 2019. A dynamic life cycle assessment of green infrastructures. Sci. Total Environ. 692, 1146–1154. https://doi.org/10.1016/j.scitotenv.2019.07.345.

Blanco, I., Schettini, E., Vox, G., 2019. Predictive model of surface temperature difference between green façades and uncovered wall in Mediterranean climatic area. Appl. Therm. Eng. 163, 114406 https://doi.org/10.1016/j.applthermaleng.2019.114406.

Bliss, D.J., Neufeld, R.D., Ries, R.J., 2009. Storm water runoff mitigation using a green roof. Environ. Eng. Sci. 26 (2), 407–418. https://doi.org/10.1089/ees.2007.0186.

Bortolini, L., Bettella, F., Zanin, G., 2020. Hydrological behaviour of extensive green roofs with native plants in the humid subtropical climate context. Water 13 (1), 44. https://doi.org/10.3390/w13010044.

Bouzouidja, R., Séré, G., Claverie, R., Ouvrard, S., Nuttens, L., Lacroix, D., 2018. Green roof aging: Quantifying the impact of substrate evolution on hydraulic performances at the lab-scale. J. Hydrol. 564, 416–423. https://doi.org/10.1016/j.jhydrol.2018.07.032.

Brink, E., Aalders, T., Ádám, D., Feller, R., Henselek, Y., Hoffmann, A., Ibe, K., Matthey-Doret, A., Meyer, M., Lucian Negrut, N., Rau, A-L., Riewerts, B., Schuckmann, L., Törnros, S., Wehrden, H., J., Abson, D., Wamsler, C., 2016. Cascades of green: a review of ecosystem-based adaptation in urban areas. Global Environ. Change 36, 111–123. https://doi.org/10.1016/j.gloenvcha.2015.11.003.

Brown, R.A., Hunt, W.F., 2012. Improving bioretention/biofiltration performance with restorative maintenance. Water Sci. Technol. 65 (2), 361–367. https://doi.org/10.2166/wst.2012.860.

Byrne, D.M., Grabowski, M.K., Benitez, A.C., Schmidt, A.R., Guest, J.S., 2017. Evaluation of life cycle assessment (LCA) for roadway drainage systems. Environ. Sci. Technol. 51 (16), 9261–9270. https://doi.org/10.1021/acs.est.7b01856.

Cameron, R.W., Taylor, J.E, Emmett, M.R., 2015. A Hedera green façade–energy performance and saving under different maritime-temperate, winter weather conditions. Build. Environ. 92, 111–121. https://doi.org/10.1016/j.buildenv.2015.04.011.

Cameron, R.W., Taylor, J.E., Emmett, M.R., 2014. What's 'cool'in the world of green façades? How plant choice influences the cooling properties of green walls. Build. Environ. 73, 198–207. https://doi.org/10.1016/j.buildenv.2013.12.005.

Campisano, A., Modica, C., 2014. Selecting time scale resolution to evaluate water saving and retention potential of rainwater harvesting tanks. Procedia Eng. 70, 218–227. https://doi.org/10.1016/j.proeng.2014.02.025.

Campos-Osorio, A., Santillán-Soto, N., García-Cueto, O.R., Lambert-Arista, A.A., Bojórquez-Morales, G., 2020. Energy and Environmental Comparison between a Concrete Wall with and without a Living Green Wall: A Case Study in Mexicali. Mexico. Sustain. 12 (13), 5265. https://doi.org/10.3390/su12135265.

Caputo, S., Schoen, V., Specht, K., Grard, B., Blythe, C., Cohen, N., Fox-Kämper, R., Hawes, J., Newell, J., Poniży, L., 2021. Applying the food-energy-water nexus approach to urban agriculture: From FEW to FEWP (Food-Energy-Water-People). Urban For. Urban Greening 58, 126934. https://doi.org/10.1016/j.ufug.2020.126934.

Cavadini, G.B., Cook, L.M., 2021. Green and cool roof choices integrated into rooftop solar energy modelling. Appl. Energy 296, 117082. https://doi.org/10.1016/j.apenergy.2021.117082.

Chàfer, M., Pérez, G., Coma, J., Cabeza, L.F., 2021. A comparative life cycle assessment between green walls and green facades in the Mediterranean continental climate. Energy Build. 249, 111236 https://doi.org/10.1016/j.enbuild.2021.111236.

Chan, F.K.S., Chen, W.Y., Gu, X., Peng, Y., Sang, Y., 2021. Transformation towards resilient sponge cities in China. Nat. Rev. Earth Environ. 1–3. https://doi.org/10.1038/s43017-021-00251-y.

Charalambous, K., Bruggeman, A., Eliades, M., Camera, C., Vassiliou, L., 2019. Stormwater retention and reuse at the residential plot level—green roof experiment and water balance computations for long-term use in cyprus. Water 11 (5), 1055. https://doi.org/10.3390/w11051055.

Clinton, N., Stuhlmacher, M., Miles, A., Uludere Aragon, N., Wagner, M., Georgescu, M., Herwig, C., Gong, P., 2018. A global geospatial ecosystem services estimate of urban agriculture. Earths Future 6 (1), 40–60. https://doi.org/10.1002/2017ef000536.

CoDyre, M., Fraser, E.D., Landman, K., 2015. How does your garden grow? An empirical evaluation of the costs and potential of urban gardening. Urban For. Urban Greening 14 (1), 72–79. https://doi.org/10.1016/j.ufug.2014.11.001.

Collins, K.A., Hunt, W.F., Hathaway, J.M., 2008. Hydrologic comparison of four types of permeable pavement and standard asphalt in eastern North Carolina. J. Hydrol. Eng. 13 (12), 1146–1157. https://doi.org/10.1061/(asce)1084-0699(2008)13:12(1146).

Coma, J., Pérez, G., de Gracia, A., Burés, S., Urrestarazu, M., Cabeza, L.F., 2017. Vertical greenery systems for energy savings in buildings: a comparative study between green walls and green facades. Build. Environ. 111, 228–237. https://doi.org/10.1016/j.buildenv.2016.11.014.

Cristiano, E., Deidda, R., Viola, F., 2021. The role of green roofs in urban Water-Energy-Food-Ecosystem nexus: a review. Sci. Total Environ. 756, 143876 https://doi.org/10.1016/j.scitotenv.2020.143876.

Dabaieh, M., Serageldin, A.A., 2020. Earth air heat exchanger, Trombe wall and green wall for passive heating and cooling in premium passive refugee house in Sweden. Energy Convers. Manag. 209, 112555 https://doi.org/10.1016/j.enconman.2020.112555.

de Oliveira, J.A.P., Bellezoni, R.A., Shih, W.Y., Bayulken, B., 2022. Innovations in Urban Green and Blue Infrastructure: tackling local and global challenges in cities. J. Clean. Prod., 132355 https://doi.org/10.1016/j.jclepro.2022.132355.

De Sousa, M.R., Montalto, F.A., Spatari, S., 2012. Using life cycle assessment to evaluate green and grey combined sewer overflow control strategies. J. Ind. Ecol. 16 (6), 901–913. https://doi.org/10.1111/j.1530-9290.2012.00534.x.

DeBusk, K.M., Wynn, T.M., 2011. Storm-water bioretention for runoff quality and quantity mitigation. J. Environ. Eng. 137 (9), 800–808. https://doi.org/10.1061/(asce)ee.1943-7870.0000388.

Denman, E.C., May, P.B., Moore, G.M., 2016. The potential role of urban forests in removing nutrients from stormwater. J. Environ. Qual. 45 (1), 207–214. https://doi.org/10.2134/jeq2015.01.0047.

Dhakal, K.P., Chevalier, L.R., 2017. Managing urban stormwater for urban sustainability: Barriers and policy solutions for green infrastructure application. J. Environ. Manag. (203), 171–181. https://doi.org/10.1016/j.jenvman.2017.07.065.

Djedjig, R., Belarbi, R., Bozonnet, E., 2017. Experimental study of green walls impacts on buildings in summer and winter under an oceanic climate. Energy Build. 150, 403–411. https://doi.org/10.1016/j.enbuild.2017.06.032.

Dong, J., Lin, M., Zuo, J., Lin, T., Liu, J., Sun, C., Luo, J., 2020. Quantitative study on the cooling effect of green roofs in a high-density urban Area—a case study of Xiamen. China. J. Clean. Prod. 255, 120152 https://doi.org/10.1016/j.jclepro.2020.120152.

dos Santos, S.M., Silva, J.F.F., dos Santos, G.C., de Macedo, P.M.T., Gavazza, S., 2019. Integrating conventional and green roofs for mitigating thermal discomfort and water scarcity in urban areas. J. Clean. Prod. 219, 639–648. https://doi.org/10.1016/j.jclepro.2019.01.068.

Duchemin, E., Wegmuller, F., Legault, A.M., 2008. Urban agriculture: multi-dimensional tools for social development in poor neighbourhoods. Field Actions Science Reports. J. Field Robot. 1 https://doi.org/10.5194/facts-2-1-2009.

Eaton, T.T., 2018. Approach and case-study of green infrastructure screening analysis for urban stormwater control. J. Environ. Manag. 209, 495–504. https://doi.org/10.1016/j.jenvman.2017.12.068.

Eckart, K., McPhee, Z., Bolisetti, T., 2017. Performance and implementation of low impact development–a review. Sci. Total Environ. 607, 413–432. https://doi.org/10.1016/j.scitotenv.2017.06.254.

Elmqvist, T., Fragkias, M., Goodness, J., Güneralp, B., Marcotullio, P.J., McDonald, R.I., Parnell, S., Schewenius, M., Sendstad, M., Seto, K.C., Wilkinson, C., 2013. Urbanization, biodiversity and ecosystem services: challenges and opportunities: a global assessment. Springer Nature, p. 755. https://doi.org/10.1007/978-94-007-7088-1_3.

Ertan, S., Çelik, R.N., 2021. The assessment of urbanization effect and sustainable drainage solutions on flood hazard by. GIS. Sustain. 13 (4), 2293. https://doi.org/10.3390/su13042293.

European Commission, 2013. Building a Green Infrastructure for Europe.

Feitosa, R.C., Wilkinson, S., 2016. Modelling green roof stormwater response for different soil depths. Landsc. Urban Plan. 153, 170–179. https://doi.org/10.1016/j.landurbplan.2016.05.007.

Fioretti, R., Palla, A., Lanza, L.G., Principi, P., 2010. Green roof energy and water related performance in the Mediterranean climate. Build. Environ. 45 (8), 1890–1904. https://doi.org/10.1016/j.buildenv.2010.03.001.

Flynn, K.M., Traver, R.G., 2013. Green infrastructure life cycle assessment: a bio-infiltration case study. Ecol. Eng. 55, 9–22. https://doi.org/10.1016/j.ecoleng.2013.01.004.

Fuhrman, J., McJeon, H., Patel, P., Doney, S.C., Shobe, W.M., Clarens, A.F., 2020. Food–energy–water implications of negative emissions technologies in a+ 1.5 C future. Nat. Clim. Change 10 (10), 920–927. https://doi.org/10.1038/s41558-020-0876-z.

Gaffin, S.R., Rosenzweig, C., Kong, A.Y., 2012. Adapting to climate change through urban green infrastructure. Nat. Clim. Change 2 (10), 704. https://doi.org/10.1038/nclimate1685.

Giese, E., Rockler, A., Shirmohammadi, A., Pavao-Zuckerman, M.A., 2019. Assessing watershed-scale stormwater green infrastructure response to climate change in Clarksburg, Maryland. J. Water Resour. Plan. Manag. 145 (10), 05019015 https://doi.org/10.1061/(asce)wr.1943-5452.0001099.

Gondhalekar, D., Ramsauer, T., 2017. Nexus city: operationalizing the urban water-energy-food nexus for climate change adaptation in Munich. Germany. Urban Clim. 19, 28–40. https://doi.org/10.1016/j.uclim.2016.11.004.

Gong, Y., Yin, D., Li, J., Zhang, X., Wang, W., Fang, X., Shi, H., Wang, Q., 2019. Performance assessment of extensive green roof runoff flow and quality control capacity based on pilot experiments. Sci. Total Environ. 687, 505–515. https://doi.org/10.1016/j.scitotenv.2019.06.100.

Gonzalez-Sosa, E., Braud, I., Piña, R.B., Loza, C.A.M., Salinas, N.M.R., Chavez, C.V., 2017. A methodology to quantify ecohydrological services of street trees. Ecohydrol. Hydrobiol. 17 (3), 190–206. https://doi.org/10.1016/j.ecohyd.2017.06.004.

Grafius, D.R., Edmondson, J.L., Norton, B.A., Clark, R., Mears, M., Leake, J.R., Corstanje, R., Harris, A.J., Warren, P.H., 2020. Estimating food production in an urban landscape. Sci. Rep. 10 (1), 1–9. https://doi.org/10.4324/9781315647692-15.

Grewal, S.S., Grewal, P.S., 2012. Can cities become self-reliant in food? Cities 29 (1), 1–11. https://doi.org/10.1016/j.cities.2011.06.003.

Haase, D., Kabisch, S., Haase, A., Andersson, E., Banzhaf, E., Baró, F., Brenck, M., Fischer, L.K., Frantzeskaki, N., Kabisch, N., Krellenberg, K., Kremer, P., Kronenberg, J., Larondelle, N., Mathey, J., Pauleit, S., Ring, I., Rink, D., Schwarz, N., Wolff, M., 2017. Greening cities–To be socially inclusive? About the alleged paradox of society and ecology in cities. Habitat Int. 64, 41–48. https://doi.org/10.1016/j.habitatint.2017.04.005.

Haase, D., Larondelle, N., Andersson, E., Artmann, M., Borgström, S., Breuste, J., Gomez-Baggethun, E., Gren, Å., Hamstead, Z., Hansen, R., Kabisch, N., Kremer, P., Langemeyer, J., Rall, E.L., McPhearson, T., Pauleit, S., Qureshi, S., Schwarz, N., Voigt, A., Wurster, D., Elmqvist, T., 2014. A quantitative review of urban ecosystem service assessments: concepts, models, and implementation. Ambio 43 (4), 413–433. https://doi.org/10.1007/s13280-014-0504-0.

Hara, Y., McPhearson, T., Sampei, Y., McGrath, B., 2018. Assessing urban agriculture potential: a comparative study of Osaka, Japan and New York city, United States. Sustain. Sci. 13 (4), 937–952. https://doi.org/10.1007/s11625-018-0535-8.

Harper, G.E., Limmer, M.A., Showalter, W.E., Burken, J.G., 2015. Nine-month evaluation of runoff quality and quantity from an experiential green roof in Missouri. USA. Ecol. Eng. 78, 127–133. https://doi.org/10.1016/j.ecoleng.2014.06.004.

He, Y., Yu, H., Ozaki, A., Dong, N., 2020. Thermal and energy performance of green roof and cool roof: a comparison study in Shanghai area. J. Clean. Prod. 267, 122205 https://doi.org/10.1016/j.jclepro.2020.122205.

Hengen, T.J., Sieverding, H.L., Stone, J.J., 2016. Lifecycle assessment analysis of engineered stormwater control methods common to urban watersheds. J. Water. Resour. Plan. Manag. 142 (7), 04016016 https://doi.org/10.1061/(asce)wr.1943-5452.0000647.

Hilten, R.N., Lawrence, T.M., Tollner, E.W., 2008. Modeling stormwater runoff from green roofs with HYDRUS-1D. J. Hydrol. 358 (3–4), 288–293. https://doi.org/10.1016/j.jhydrol.2008.06.010.

Hoyer, J., Dickhaut, W., Kronawitter, L., Weber, B., 2011. Water sensitive urban design. JOVIS Verlag GmBH.

Huang, J., Ridoutt, B.G., Zhang, H., Xu, C., Chen, F., 2014. Water footprint of cereals and vegetables for the Beijing market: comparison between local and imported supplies. J. Ind. Ecol. 18 (1), 40–48. https://doi.org/10.1111/jiec.12037.

Huang, Y., Liu, Y., Liu, Y., Li, H., Knievel, J.C., 2019. Mechanisms for a record-breaking rainfall in the coastal metropolitan city of Guangzhou, China: Observation analysis and nested very large eddy simulation with the WRF model. J. Geophys. Res.: Atmos. 124 (3), 1370–1391. https://doi.org/10.1029/2018jd029668.

IPCC, 2014. Summary for policymakers in: climate change 2014: impacts, adaptation, and vulnerability. part a: global and sectoral aspects. In: Contribution of Working Group II to the Fifth Assessment Report of the Intergovernmental Panel on Climate Change.

Jahanfar, A., Sleep, B., Drake, J., 2018. Energy and carbon-emission analysis of integrated green-roof photovoltaic systems: probabilistic approach. J. Infrastruct. Syst. 24 (1), 04017044 https://doi.org/10.1061/(asce)is.1943-555x.0000399.

Jeong, H., Broesicke, O.A., Drew, B., Li, D., Crittenden, J.C., 2016. Life cycle assessment of low impact development technologies combined with conventional centralized water systems for the City of Atlanta. Georgia. Front. Environ. Sci. Eng. 10 (6), 1–13. https://doi.org/10.1007/s11783-016-0851-0.

Jing, R., Hastings, A., Guo, M., 2020. Sustainable design of urban rooftop food-energy-land nexus. iScience 23 (11), 101743. https://doi.org/10.1016/j.isci.2020.101743.

Jing, R., Li, Y., Wang, M., Chachuat, B., Lin, J., Guo, M., 2021. Coupling biogeochemical simulation and mathematical optimisation towards eco-industrial energy systems design. Appl. Energy 290, 116773. https://doi.org/10.1016/j.apenergy.2021.116773.

Jung, J.W., Kim, Y.S., Hong, S.J., Kwon, H.S., Kim, J.W., Kim, H.S., 2014. Effectiveness analysis of artificial wetland for flood reduction. J. Korean Soc. Haz. Mitig. 14 (4), 369–378. https://doi.org/10.9798/kosham.2014.14.4.369.

Kavehei, E., Jenkins, G.A., Adame, M.F., Lemckert, C., 2018. Carbon sequestration potential for mitigating the carbon footprint of green stormwater infrastructure. Renew. Sustain. Energy Rev. 94, 1179–1191. https://doi.org/10.1016/j.rser.2018.07.002.

Khurelbaatar, G., van Afferden, M., Ueberham, M., Stefan, M., Geyler, S., Müller, R.A., 2021. Management of Urban Stormwater at Block-Level (MUST-B): A New Approach for Potential Analysis of Decentralized Stormwater Management Systems. Water 13 (3), 378. https://doi.org/10.3390/w13030378.

Koc, C.B., Osmond, P., Peters, A., 2018. Evaluating the cooling effects of green infrastructure: A systematic review of methods, indicators and data sources. Sol. Energy 166, 486–508. https://doi.org/10.1016/j.solener.2018.03.008.

Kong, F., Sun, C., Liu, F., Yin, H., Jiang, F., Pu, Y., Cavan, G., Skelhorn, C., Middel, A., Dronova, I., 2016. Energy saving potential of fragmented green spaces due to their temperature regulating ecosystem services in the summer. Appl. Energy 183, 1428–1440. https://doi.org/10.1016/j.apenergy.2016.09.070.

Kosareo, L., Ries, R., 2007. Comparative environmental life cycle assessment of green roofs. Build. Environ. 42 (7), 2606–2613. https://doi.org/10.1016/j.buildenv.2006.06.019.

Koyama, T., Yoshinaga, M., Maeda, K.I., Yamauchi, A., 2015. Transpiration cooling effect of climber greenwall with an air gap on indoor thermal environment. Ecol. Eng. 83, 343–353. https://doi.org/10.1016/j.ecoleng.2015.06.015.

Kraxner, F., Aoki, K., Kindermann, G., Leduc, S., Albrecht, F., Liu, J., Yamagata, Y., 2016. Bioenergy and the city–what can urban forests contribute? Appl. Energy 165, 990–1003. https://doi.org/10.1016/j.apenergy.2015.12.121.

Kremer, P, Hamstead, Z, Haase, D, McPhearson, T, Frantzeskaki, N, Andersson, E, Kabisch, N, Larondelle, N, Rall, EL, Voigt, A, Baró, F., 2016. Key insights for the future of urban ecosystem services research. Ecol. Soc. 21 (2), 29. https://doi.org/10.5751/ES-08445-210229.

Kristvik, E., Johannessen, B.G., Muthanna, T.M., 2019. Temporal downscaling of IDF curves applied to future performance of local stormwater measures. Sustain 11 (5), 1231. https://doi.org/10.3390/su11051231.

Kulak, M., Graves, A., Chatterton, J., 2013. Reducing greenhouse gas emissions with urban agriculture: A Life Cycle Assessment perspective. Landsc. Urban Plan. 111, 68–78. https://doi.org/10.1016/j.landurbplan.2012.11.007.

Kuoppamäki, K., Hagner, M., Lehvävirta, S., Setälä, H., 2016. Biochar amendment in the green roof substrate affects runoff quality and quantity. Ecol. Eng. 88, 1–9. https://doi.org/10.1016/j.ecoleng.2015.12.010.

Kuronuma, T., Watanabe, H., Ishihara, T., Kou, D., Toushima, K., Ando, M., Shindo, S., 2018. CO2 payoff of extensive green roofs with different vegetation species. Sustain 10 (7), 2256. https://doi.org/10.3390/su10072256.

Lafontaine-Messier, M., Gélinas, N., Olivier, A., 2016. Profitability of food trees planted in urban public green areas. Urban For. Urban Greening 16, 197–207. https://doi.org/10.1016/j.ufug.2016.02.013.

Lamnatou, C., Chemisana, D., 2014. Photovoltaic-green roofs: a life cycle assessment approach with emphasis on warm months of Mediterranean climate. J. Clean. Prod. 72, 57–75. https://doi.org/10.1016/j.jclepro.2014.03.006.

Lee, G.G., Lee, H.W., Lee, J.H., 2015. Greenhouse gas emission reduction effect in the transportation sector by urban agriculture in Seoul. Korea. Landsc. Urban Plan. 140, 1–7. https://doi.org/10.1016/j.landurbplan.2015.03.012.

Lee, L.S., Jim, C.Y., 2020. Thermal-irradiance behaviours of subtropical intensive green roof in winter and landscape-soil design implications. Energy Build. 209, 109692 https://doi.org/10.1016/j.enbuild.2019.109692.

Lee, S.W., Kim, R., 2016. Application of Benefit Assessment to Infiltration Storage Tank and Permeable Pavement Demonstrated in Seoul Metropolitan. Korea. Int. J. Hybrid Inf. Technol. 9 (9), 411–422. https://doi.org/10.14257/ijhit.2016.9.9.37.

Li, J., Li, F., Li, H., Guo, C., Dong, W., 2019. Analysis of rainfall infiltration and its influence on groundwater in rain gardens. Environ. Sci. Pollut. Res. 26 (22), 22641–22655. https://doi.org/10.1007/s11356-019-05622-z.

Li, J., Zhang, B., Mu, C., Chen, L., 2018. Simulation of the hydrological and environmental effects of a sponge city based on MIKE FLOOD. Environ. Earth Sci. 77 (2), 1–16. https://doi.org/10.1007/s12665-018-7236-6.

Li, Y.H., Tung, C.P., Chen, P.Y., 2017. Stormwater management toward water supply at the community scale—A case study in northern Taiwan. Sustain. 9 (7), 1206. https://doi.org/10.3390/su9071206.

Liu, D., Zou, C., Xu, M., 2019. Environmental, ecological, and economic benefits of biofuel production using a constructed wetland: a case study in China. Int. J. Environ. Res. Public Health. 16 (5), 827. https://doi.org/10.3390/ijerph16050827.
Liu, J., Hull, V., Godfray, H.C.J., Tilman, D., Gleick, P., Hoff, H., Pahl-Wostl, C., Xu, Z., Chung, M.G., Sun, J., Li, S., 2018. Nexus approaches to global sustainable development. Nat. Sustain. 1 (9), 466–476. https://doi.org/10.4324/9781003000365.
Liu, L., Sun, L., Niu, J., Riley, W.J., 2020. Modeling green roof potential to mitigate urban flooding in a Chinese City. Water 12 (8), 2082. https://doi.org/10.3390/w12082082.
Liu, Q., 2016. Interlinking climate change with water-energy-food nexus and related ecosystem processes in California case studies. Ecol. Process. 5 (1), 1–14. https://doi.org/10.1186/s13717-016-0058-0.
Liu, W., Chen, W., Peng, C., 2014. Assessing the effectiveness of green infrastructures on urban flooding reduction: a community scale study. Ecol. Modell. 291, 6–14. https://doi.org/10.1016/j.ecolmodel.2014.07.012.
Luan, Q., Fu, X., Song, C., Wang, H., Liu, J., Wang, Y., 2017. Runoff effect evaluation of LID through SWMM in typical mountainous, low-lying urban areas: a case study in China. Water 9 (6), 439. https://doi.org/10.3390/w9060439.
Lucke, T., Nichols, P.W., 2015. The pollution removal and stormwater reduction performance of street-side bioretention basins after ten years in operation. Sci. Total Environ. 536, 784–792. https://doi.org/10.1016/j.scitotenv.2015.07.142.
Lund, N.S.V., Borup, M., Madsen, H., Mark, O., Arnbjerg-Nielsen, K., Mikkelsen, P.S., 2019. Integrated stormwater inflow control for sewers and green structures in urban landscapes. Nat. Sustain. 2 (11), 1003–1010. https://doi.org/10.1038/s41893-019-0392-1.
Lundholm, J., MacIvor, J.S., MacDougall, Z., Ranalli, M., 2010. Plant species and functional group combinations affect green roof ecosystem functions. PLoS One 5 (3), e9677. https://doi.org/10.3410/f.3264976.2951082.
MacRae, R., Gallant, E., Patel, S., Michalak, M., Bunch, M., Schaffner, S., 2010. Could Toronto provide 10% of its fresh vegetable requirements from within its own boundaries? Matching consumption requirements with growing spaces. J. Agri. Food Syst. Commun Develop. 1 (2), 105–127. https://doi.org/10.5304/jafscd.2010.012.008.
Mahmoud, A., Alam, T., Sanchez, A., Guerrero, J., Oraby, T., Ibrahim, E., Jones, K.D., 2020. Stormwater runoff quality and quantity from permeable and traditional pavements in semiarid South Texas. J. Environ. Eng. 146 (6), 05020001 https://doi.org/10.1061/(asce)ee.1943-7870.0001685.
Manso, M., Castro-Gomes, J., Paulo, B., Bentes, I., Teixeira, C.A., 2018. Life cycle analysis of a new modular greening system. Sci. Total Environ. 627, 1146–1153. https://doi.org/10.1016/j.scitotenv.2018.01.198.
McClintock, N., Cooper, J., Khandeshi, S., 2013. Assessing the potential contribution of vacant land to urban vegetable production and consumption in Oakland. California. Landsc. Urban Plan. 111, 46–58. https://doi.org/10.1016/j.landurbplan.2012.12.009.
McDougall, R., Kristiansen, P., Rader, R., 2019. Small-scale urban agriculture results in high yields but requires judicious management of inputs to achieve sustainability. Proc. Natl. Acad. Sci. U. S. A. 116 (1), 129–134. https://doi.org/10.1073/pnas.1809707115.
McLain, R., Poe, M., Hurley, P.T., Lecompte-Mastenbrook, J., Emery, M.R., 2012. Producing edible landscapes in Seattle's urban forest. Urban For. Urban Greening 11 (2), 187–194. https://doi.org/10.1016/j.ufug.2011.12.002.
Mell, I.C., 2017. Green infrastructure: reflections on past, present and future praxis. Landsc. Res. 42 (2), 135–145. https://doi.org/10.1080/01426397.2016.1250875.
Melo, F.P., Parry, L., Brancalion, P.H., Pinto, S.R., Freitas, J., Manhães, A.P., Meli, P., Ganade, G., Chazdon, R.L., 2021. Adding forests to the water–energy–food nexus. Nature. Sustain. 4 (2), 85–92. https://doi.org/10.1038/s41893-020-00608-z.
Meng, F., Liu, G., Chang, Y., Su, M., Hu, Y., Yang, Z., 2019a. Quantification of urban water-carbon nexus using disaggregated input-output model: a case study in Beijing (China). Energy 171, 403–418. https://doi.org/10.1016/j.energy.2019.01.013.
Meng, F., Liu, G., Liang, S., Su, M., Yang, Z., 2019b. Critical review of the energy-water-carbon nexus in cities. Energy 171, 1017–1032. https://doi.org/10.1016/j.energy.2019.01.048.
Meng, F., Wang, D., Meng, X., Li, H., Liu, G., Yuan, Q., Hu, Y., Zhang, Y., 2022. Mapping urban energy–water–land nexus within a multiscale economy: A case study of four megacities in China. Energy 239 (122038). https://doi.org/10.1016/j.energy.2021.122038.
Miller-Robbie, L., Ramaswami, A., Amerasinghe, P., 2017. Wastewater treatment and reuse in urban agriculture: exploring the food, energy, water, and health nexus in Hyderabad. India. Environ. Res. Lett. 12 (7), 075005 https://doi.org/10.1088/1748-9326/aa6bfe.
Monteiro, M.V., Doick, K.J., Handley, P., Peace, A., 2016. The impact of greenspace size on the extent of local nocturnal air temperature cooling in London. Urban For. Urban Greening 16, 160–169. https://doi.org/10.1016/j.ufug.2016.02.008.
Moody, S.S., Sailor, D.J., 2013. Development and application of a building energy performance metric for green roof systems. Energy Build. 60, 262–269. https://doi.org/10.1016/j.enbuild.2013.02.002.
Moore, T.L., Hunt, W.F., 2013. Predicting the carbon footprint of urban stormwater infrastructure. Ecol. Eng. 58, 44–51. https://doi.org/10.1016/j.ecoleng.2013.06.021.
Moreno, R.A.R., 2011. Vivienda y consumo de energía eléctrica en zonas áridas: el caso de Mexicali. Universidad Autónoma de Baja California. https://doi.org/10.21158/01208160.n72.2012.570.
Nadal, A., Rodríguez-Cadena, D., Pons, O., Cuerva, E., Josa, A., Rieradevall, J., 2019. Feasibility assessment of rooftop greenhouses in Latin America. The case study of a social neighborhood in Quito, Ecuador. Urban For. Urban Greening 44, 126389. https://doi.org/10.1016/j.ufug.2019.126389.
Nagengast, A., Hendrickson, C., Matthews, H.S., 2013. Variations in photovoltaic performance due to climate and low-slope roof choice. Energy Build. 64, 493–502. https://doi.org/10.1016/j.enbuild.2013.05.009.
Newcomer, M.E., Gurdak, J.J., Sklar, L.S., Nanus, L., 2014. Urban recharge beneath low impact development and effects of climate variability and change. Water Resour. Res. 50 (2), 1716–1734. https://doi.org/10.1002/2013wr014282.
Nou, C., Charoenkit, S., 2020. The potential of green infrastructure (gi) for reducing stormwater runoff in a Phnom Penh neighborhood. Geogr. Tech. 15 (1), 112–123. https://doi.org/10.21163/GT_2020.151.10.
Nurmatov, N., Leon Gomez, D.A., Hensgen, F., Bühle, L., Wachendorf, M., 2016. High-quality solid fuel production from leaf litter of urban street trees. Sustain 8 (12), 1249. https://doi.org/10.3390/su8121249.
O'Sullivan, A.D., Wicke, D., Hengen, T.J., Sieverding, H.L., Stone, J.J., 2015. Life Cycle Assessment modelling of stormwater treatment systems. J. Environ. Manag. 149, 236–244. https://doi.org/10.1016/j.jenvman.2014.10.025.
Oquendo-Di Cosola, V., Olivieri, F., Ruiz-García, L., Bacenetti, J., 2020. An environmental life cycle assessment of living wall systems. J. Environ. Manag. 254, 109743 https://doi.org/10.1016/j.jenvman.2019.109743.
Orsini, F., Gasperi, D., Marchetti, L., Piovene, C., Draghetti, S., Ramazzotti, S., Bazzocchi, G., Gianquinto, G., 2014. Exploring the production capacity of rooftop gardens (RTGs) in urban agriculture: the potential impact on food and nutrition security, biodiversity and other ecosystem services in the city of Bologna. Food Sec. 6 (6), 781–792. https://doi.org/10.1007/s12571-014-0389-6.
Ottelé, M., Perini, K., Fraaij, A.L.A., Haas, E.M., Raiteri, R., 2011. Comparative life cycle analysis for green façades and living wall systems. Energy Build. 43 (12), 3419–3429. https://doi.org/10.1016/j.enbuild.2011.09.010.
Ouldboukhitine, S.E., Belarbi, R., Sailor, D.J., 2014. Experimental and numerical investigation of urban street canyons to evaluate the impact of green roof inside and outside buildings. Appl. Energy 114, 273–282. https://doi.org/10.1016/j.apenergy.2013.09.073.
Pan, L., Chu, L.M., 2016. Energy saving potential and life cycle environmental impacts of a vertical greenery system in Hong Kong: a case study. Build. Environ. 96, 293–300. https://doi.org/10.1016/j.buildenv.2015.06.033.
Park, J., Kim, J.H., Lee, D.K., Park, C.Y., Jeong, S.G., 2017. The influence of small green space type and structure at the street level on urban heat island mitigation. Urban For. Urban Greening 21, 203–212. https://doi.org/10.1016/j.ufug.2016.12.005.
Peng, L.L., Jiang, Z., Yang, X., Wang, Q., He, Y., Chen, S.S., 2020. Energy savings of block-scale façade greening for different urban forms. Appl. Energy 279, 115844. https://doi.org/10.1016/j.apenergy.2020.115844.
Peng, L.L., Jim, C.Y., 2013. Green-roof effects on neighborhood microclimate and human thermal sensation. Energies 6 (2), 598–618. https://doi.org/10.3390/en6020598.
Peng, L.L., Jim, C.Y., 2015. Economic evaluation of green-roof environmental benefits in the context of climate change: The case of Hong Kong. Urban For. Urban Greening 14 (3), 554–561. https://doi.org/10.1016/j.ufug.2015.05.006.
Pérez, G., Coma, J., Sol, S., Cabeza, L.F., 2017. Green facade for energy savings in buildings: The influence of leaf area index and facade orientation on the shadow effect. Appl. Energy 187, 424–437. https://doi.org/10.1016/j.apenergy.2016.11.055.
Pitman, S.D., Daniels, C.B., Ely, M.E., 2015. Green infrastructure as life support: Urban nature and climate change. T. Roy Soc. South Aust. 139 (1), 97–112. https://doi.org/10.1080/03721426.2015.1035219.
Pourais, J., Duchemin, E., Aubry, C., 2015. Products from urban collective gardens: Food for thought or for consumption? Insights from Paris and Montreal. J. Agri. Food Syst. Commun Develop. 5 (2), 175–199. https://doi.org/10.1007/s10460-015-9606-y.
Pulighe, G., Lupia, F., 2019. Multitemporal geospatial evaluation of urban agriculture and (non)-sustainable food self-provisioning in Milan. Italy. Sustain. 11 (7), 1846. https://doi.org/10.3390/su11071846.
Pushkar, S., 2019. Modeling the substitution of natural materials with industrial byproducts in green roofs using life cycle assessments. J. Clean. Prod. 227, 652–661. https://doi.org/10.1016/j.jclepro.2019.04.237.
Ramaswami, A., Boyer, D., Nagpure, A.S., Fang, A., Bogra, S., Bakshi, B., Cohen, E., Rao-Ghorpade, A., 2017. An urban systems framework to assess the trans-boundary food-energy-water nexus: implementation in Delhi. India. Environ. Res. Lett. 12 (2), 025008 https://doi.org/10.1088/1748-9326/aa5556.
Rasul, G., Sharma, B., 2016. The nexus approach to water–energy–food security: an option for adaptation to climate change. Clim. Policy. 16 (6), 682–702. https://doi.org/10.1080/14693062.2015.1029865.
Ringler, C., Bhaduri, A., Lawford, R., 2013. The nexus across water, energy, land and food (WELF): potential for improved resource use efficiency? Curr. Opin. Environ. Sustain. 5 (6), 617–624. https://doi.org/10.1016/j.cosust.2013.11.002.
Riolo, F., 2019. The social and environmental value of public urban food forests: The case study of the Picasso Food Forest in Parma, Italy. Urban For. Urban Greening 45, 126225. https://doi.org/10.1016/j.ufug.2018.10.002.
Roth, J.J., Passig, F.H., Zanetti, F.L., Pelissari, C., Sezerino, P.H., Nagalli, A., Carvalho, K. Q., 2021. Influence of the flooded time on the performance of a tidal flow constructed wetland treating urban stream water. Sci. Total Environ. 758, 143652 https://doi.org/10.1016/j.scitotenv.2020.143652.
Rupasinghe, H.T., Halwatura, R.U., 2020. Benefits of implementing vertical greening in tropical climates. Urban For. Urban Greening 53, 126708. https://doi.org/10.1016/j.ufug.2020.126708.
Russo, A., Cirella, G.T., 2019. Edible urbanism 5.0. Palgrave Commun. 5 (1), 1–9. https://doi.org/10.3390/ifou-a011.
Saha, M., Eckelman, M.J., 2017. Growing fresh fruits and vegetables in an urban landscape: a geospatial assessment of ground level and rooftop urban agriculture

potential in Boston, USA. Landsc. Urban Plan 165, 130–141. https://doi.org/10.1016/j.landurbplan.2017.04.015.
Saiz, S., Kennedy, C., Bass, B., Pressnail, K., 2006. Comparative life cycle assessment of standard and green roofs. Environ. Sci. Technol. 40 (13), 4312–4316. https://doi.org/10.1021/es0517522.
Salvador, D.S., Toboso-Chavero, S., Nadal, A., Gabarrell, X., Rieradevall, J., da Silva, R. S., 2019. Potential of technology parks to implement Roof Mosaic in Brazil. J. Clean. Prod. 235, 166–177. https://doi.org/10.1016/j.jclepro.2019.06.214.
Sánchez-Reséndiz, J.A., Ruiz-García, L., Olivieri, F., Ventura-Ramos Jr, E., 2018. Experimental assessment of the thermal behavior of a living wall system in semi-arid environments of central Mexico. Energy Build. 174, 31–43. https://doi.org/10.1016/j.enbuild.2018.05.060.
Sanjuan-Delmás, D., Llorach-Massana, P., Nadal, A., Ercilla-Montserrat, M., Muñoz, P., Montero, J.I., Alejandro, J., Gabarrell, X., Rieradevall, J., 2018. Environmental assessment of an integrated rooftop greenhouse for food production in cities. J. Clean. Prod. 177, 326–337. https://doi.org/10.1016/j.jclepro.2017.12.147.
Sanyé-Mengual, E., Oliver-Solà, J., Montero, J.I., Rieradevall, J., 2015. An environmental and economic life cycle assessment of rooftop greenhouse (RTG) implementation in Barcelona, Spain. Assessing new forms of urban agriculture from the greenhouse structure to the final product level. Int. J. Life Cycle Assess. 20 (3), 350–366. https://doi.org/10.1007/s11367-014-0836-9.
Sanyé-Mengual, E., Cerón-Palma, I., Oliver-Solà, J., Montero, J.I., Rieradevall, J., 2013. Environmental analysis of the logistics of agricultural products from roof top greenhouses in Mediterranean urban areas. J. Sci. Food Agri. 93 (1), 100–109. https://doi.org/10.1002/jsfa.5736.
Sendo, T., Kanechi, M., Uno, Y., Inagaki, N., 2010. Evaluation of growth and green coverage of ten ornamental species for planting as urban rooftop greening. J. Jpn Soc. Horti Sci. 79 (1), 69–76. https://doi.org/10.2503/jjshs1.79.69.
Shafique, M., Azam, A., Rafiq, M., Ateeq, M., Luo, X., 2020. An overview of life cycle assessment of green roofs. J. Clean. Prod. 250, 119471 https://doi.org/10.1016/j.jclepro.2019.119471.
Shah, A.M., Liu, G., Huo, Z., Yang, Q., Zhang, W., Meng, F., Yao, L., Ulgiati, S., 2022. Assessing environmental services and disservices of urban street trees. an application of the emergy accounting. Resour. Conserv. Recycl. 186, 106563. https://doi.org/10.1016/j.resconrec.2022.106563.
Shah, A.M., Liu, G., Meng, F., Yang, Q., Xue, J., Dumontet, S., Passaro, R., Casazza, M., 2021. A Review of Urban Green and Blue Infrastructure from the Perspective of Food-Energy-Water Nexus. Energies 14 (15), 4583. https://doi.org/10.3390/en14154583.
Shannak, S., Mabrey, D., Vittorio, M., 2018. Moving from theory to practice in the water–energy–food nexus: an evaluation of existing models and frameworks. Water-Energy Nexus 1 (1), 17–25. https://doi.org/10.1016/j.wen.2018.04.001.
Shashua-Bar, L., Pearlmutter, D., Erell, E., 2011. The influence of trees and grass on outdoor thermal comfort in a hot-arid environment. Int. J. Climatol. 31 (10), 1498–1506. https://doi.org/10.1002/joc.2177.
Shi, Y., Ge, Y., Chang, J., Shao, H., Tang, Y., 2013. Garden waste biomass for renewable and sustainable energy production in China: potential, challenges and development. Renew. Sustain. Energy Rev. 22, 432–437. https://doi.org/10.1016/j.rser.2013.02.003.
Sioen, G.B., Sekiyama, M., Terada, T., Yokohari, M., 2017. Post-disaster food and nutrition from urban agriculture: a self-sufficiency analysis of Nerima Ward. Tokyo. Int. J. Environ. Res. Public Health. 14 (7), 748. https://doi.org/10.3390/ijerph14070748.
Snir, K., Pearlmutter, D., Erell, E., 2016. The moderating effect of water-efficient ground cover vegetation on pedestrian thermal stress. Landsc. Urban Plan. 152, 1–12. https://doi.org/10.1016/j.landurbplan.2016.04.008.
Song, P., Guo, J., Xu, E., Mayer, A.L., Liu, C., Huang, J., Tian, G., Kim, G., 2020. Hydrological effects of urban green space on stormwater runoff reduction in Luohe. China. Sustain. 12 (16), 6599. https://doi.org/10.3390/su12166599.
Spatari, S., Yu, Z., Montalto, F.A., 2011. Life cycle implications of urban green infrastructure. Environ. Pollut. 159 (8–9), 2174–2179. https://doi.org/10.1016/j.envpol.2011.01.015.
Springer, T.L., 2012. Biomass yield from an urban landscape. Biomass Bioenerg. 37, 82–87. https://doi.org/10.1016/j.biombioe.2011.12.029.
Stovin, V., Vesuviano, G., Kasmin, H., 2012. The hydrological performance of a green roof test bed under UK climatic conditions. J. Hydrol. 414, 148–161. https://doi.org/10.1016/j.jhydrol.2011.10.022.
Taylor, J.R., Lovell, S.T., 2012. Mapping public and private spaces of urban agriculture in Chicago through the analysis of high-resolution aerial images in Google Earth. Landsc. Urban Plan. 108 (1), 57–70. https://doi.org/10.1016/j.landurbplan.2012.08.001.
Theodosiou, T., Aravantinos, D., Tsikaloudaki, K., 2014. Thermal behaviour of a green vs. a conventional roof under Mediterranean climate conditions. J. Renew. Sustain. Energy. 33 (1), 227–241. https://doi.org/10.1080/14786451.2013.772616.
Toboso-Chavero, S., Nadal, A., Petit-Boix, A., Pons, O., Villalba, G., Gabarrell, X., Josa, A., Rieradevall, J., 2019. Towards productive cities: environmental assessment of the food-energy-Water Nexus of the urban roof mosaic. J. Ind. Ecol. 23 (4), 767–780. https://doi.org/10.1111/jiec.12829.
Todeschi, V., Mutani, G., Baima, L., Nigra, M., Robiglio, M., 2020. Smart solutions for sustainable cities—The re-coding experience for harnessing the potential of urban rooftops. Appl. Sci. 10 (20), 7112. https://doi.org/10.3390/app10207112.
Tu, M.C., Traver, R., 2019. Water table fluctuation from green infrastructure sidewalk planters in Philadelphia. J. Irrig. Drain. Eng. 145 (2), 05018008 https://doi.org/10.1061/(asce)ir.1943-4774.0001369.
United Nations, 2019. World Urbanization Prospects 2018. Department of Economic and Social Affairs, Population Division, United Nations: New York City, NY, United States of America.
Vijayaraghavan, K., Joshi, U.M., Balasubramanian, R., 2012. A field study to evaluate runoff quality from green roofs. Water Res. 46 (4), 1337–1345. https://doi.org/10.1016/j.watres.2011.12.050.
Vineyard, D., Ingwersen, W.W., Hawkins, T.R., Xue, X., Demeke, B., Shuster, W., 2015. Comparing green and grey infrastructure using life cycle cost and environmental impact: a rain garden case study in Cincinnati. OH. J. Am. Water Resour. Assoc. 51 (5), 1342–1360. https://doi.org/10.1111/1752-1688.12320.
Wang, R., Eckelman, M.J., Zimmerman, J.B., 2013. Consequential environmental and economic life cycle assessment of green and gray stormwater infrastructures for combined sewer systems. Environ. Sci. Technol. 47 (19), 11189–11198. https://doi.org/10.1021/es4026547.
Wang, Y.C., Ko, C.H., Chang, F.C., Chen, P.Y., Liu, T.F., Sheu, Y.S., Shih, T.L., Teng, C.J., 2011. Bioenergy production potential for aboveground biomass from a subtropical constructed wetland. Biomass Bioenerg. 35 (1), 50–58. https://doi.org/10.1016/j.biombioe.2010.08.032.
Wang, Y., Akbari, H., 2016. The effects of street tree planting on Urban Heat Island mitigation in Montreal. Sustain. Cities Soc. 27, 122–128. https://doi.org/10.1016/j.scs.2016.04.013.
Wang, Y., Ni, Z., Hu, M., Li, J., Wang, Y., Lu, Z., Chen, S., Xia, B., 2020. Environmental performances and energy efficiencies of various urban green infrastructures: A life-cycle assessment. J. Clean. Prod. 248, 119244 https://doi.org/10.1016/j.jclepro.2019.119244.
Wei, T., Jim, C.Y., Chen, A., Li, X., 2020. Adjusting soil parameters to improve green roof winter energy performance based on neural-network modeling. Energy Rep. 6, 2549–2559. https://doi.org/10.1016/j.egyr.2020.09.012.
Weidner, T., Yang, A., Hamm, M.W., 2019. Consolidating the current knowledge on urban agriculture in productive urban food systems: Learnings, gaps and outlook. J. Clean. Prod. 1637–1655. https://doi.org/10.1016/j.jclepro.2018.11.004.
Wiedmann, T., Minx, J., 2008. A definition of 'carbon footprint. Ecol Econ Res Tren 1 (2008), 1–11.
Winston, R.J., Dorsey, J.D., Hunt, W.F., 2016. Quantifying volume reduction and peak flow mitigation for three bioretention cells in clay soils in northeast Ohio. Sci. Total Environ. 553, 83–95. https://doi.org/10.1016/j.scitotenv.2016.02.081.
Wong, I., Baldwin, A.N., 2016. Investigating the potential of applying vertical green walls to high-rise residential buildings for energy-saving in sub-tropical region. Build. Environ. 97, 34–39. https://doi.org/10.1016/j.buildenv.2015.11.028.
Wong, N.H., Tan, A.Y.K., Tan, P.Y., Wong, N.C., 2009. Energy simulation of vertical greenery systems. Energy Build. 41 (12), 1401–1408. https://doi.org/10.1016/j.enbuild.2009.08.010.
Wong, N.H., Tan, C.L., Kolokotsa, D.D., Takebayashi, H., 2021. Greenery as a mitigation and adaptation strategy to urban heat. Nat. Rev. Earth Environ. 2 (3), 166–181. https://doi.org/10.1038/s43017-020-00129-5.
Xiao, L., Chen, Z., Zhou, F., ben Hammouda, S., Zhu, Y., 2020. Modeling of a Surface Flow Constructed Wetland Using the HEC-RAS and QUAL2K Models: a Comparative Analysis. Wetlands 40 (6), 2235–2245. https://doi.org/10.1007/s13157-020-01349-7.
Xing, Q., Hao, X., Lin, Y., Tan, H., Yang, K., 2019. Experimental investigation on the thermal performance of a vertical greening system with green roof in wet and cold climates during winter. Energy Build. 183, 105–117. https://doi.org/10.1016/j.enbuild.2018.10.038.
Xu, C., Liu, Z., Chen, Z., Zhu, Y., Yin, D., Leng, L., Jia, H., Zhang, X., Xia, J., Fu, G., 2021. Environmental and economic benefit comparison between coupled grey-green infrastructure system and traditional grey one through a life cycle perspective. Resour. Conserv. Recycl. 174, 105804 https://doi.org/10.1016/j.resconrec.2021.105804.
Xue, Z., Hou, G., Zhang, Z., Lyu, X., Jiang, M., Zou, Y., Shen, X., Wang, J., Liu, X., 2019. Quantifying the cooling-effects of urban and peri-urban wetlands using remote sensing data: Case study of cities of Northeast China. Landsc. Urban Plan. 182, 92–100. https://doi.org/10.1016/j.landurbplan.2018.10.015.
Yang, B., Goodwin, A.A., Dupont, R.R., Rycewicz-Borecki, M., 2014. Form-based Variables for Stormwater Quality Performance. Urban Plan. Des. Res. 2, 14–19. https://doi.org/10.4324/9781315636825-10.
Yang, J., Bou-Zeid, E., 2019. Scale dependence of the benefits and efficiency of green and cool roofs. Landsc. Urban Plan. 185, 127–140. https://doi.org/10.1016/j.landurbplan.2019.02.004.
Yang, Y., Campbell, J.E., 2017. Improving attributional life cycle assessment for decision support: The case of local food in sustainable design. J. Clean. Prod. 145, 361–366. https://doi.org/10.1016/j.jclepro.2017.01.020.
Yao, L., Wu, Z., Wang, Y., Sun, S., Wei, W., Xu, Y., 2020. Does the spatial location of green roofs affects runoff mitigation in small urbanized catchments? J. Environ. Manag. 268, 110707 https://doi.org/10.1016/j.jenvman.2020.110707.
Yu, Z., Chen, T., Yang, G., Sun, R., Xie, W., Vejre, H., 2020. Quantifying seasonal and diurnal contributions of urban landscapes to heat energy dynamics. Appl. Energy 264, 114724. https://doi.org/10.1016/j.apenergy.2020.114724.
Zhang, B., Li, N., Wang, S., 2015. Effect of urban green space changes on the role of rainwater runoff reduction in Beijing. China. Landsc. Urban Plan. 140, 8–16. https://doi.org/10.1016/j.landurbplan.2015.03.014.
Zhang, G., He, B.J., Dewancker, B.J., 2020. The maintenance of prefabricated green roofs for preserving cooling performance: A field measurement in the subtropical city of Hangzhou. China. Sustain. Cities Soc. 61, 102314 https://doi.org/10.1016/j.scs.2020.102314.

Zhang, J., Peralta, R.C., 2019. Estimating infiltration increase and runoff reduction due to green infrastructure. J. Water Clim. Chang. 10 (2), 237–242. https://doi.org/10.2166/wcc.2018.354.

Zhang, P., Zhang, L., Chang, Y., Xu, M., Hao, Y., Liang, S., Yang, Z., Wang, C., 2019. Food-energy-water (FEW) nexus for urban sustainability: A comprehensive review. Resour. Conserv. Recycl. 142, 215–224. https://doi.org/10.1016/j.resconrec.2018.11.018.

Zheng, Y., Weng, Q., 2020. Modeling the effect of green roof systems and photovoltaic panels for building energy savings to mitigate climate change. Remote Sens. 12 (15), 2402. https://doi.org/10.3390/rs12152402.

Zhu, Z., Zhou, D., Wang, Y., Ma, D., Meng, X., 2021. Assessment of urban surface and canopy cooling strategies in high-rise residential communities. J. Clean. Prod. 288, 125599 https://doi.org/10.1016/j.jclepro.2020.125599.

Ziter, C.D., Pedersen, E.J., Kucharik, C.J., Turner, M.G., 2019. Scale-dependent interactions between tree canopy cover and impervious surfaces reduce daytime urban heat during summer. Proc. Natl. Acad. Sci. U. S. A. 116 (15), 7575–7580. https://doi.org/10.1073/pnas.1817561116.

Žuvela-Aloise, M., Andre, K., Schwaiger, H., Bird, D.N., Gallaun, H., 2018. Modelling reduction of urban heat load in Vienna by modifying surface properties of roofs. Theor. Appl. Climatol. 131 (3), 1005–1018. https://doi.org/10.1007/s00704-016-2024-2.

Žuvela-Aloise, M., Koch, R., Buchholz, S., Früh, B., 2016. Modelling the potential of green and blue infrastructure to reduce urban heat load in the city of Vienna. Clim. Change 135 (3), 425–438. https://doi.org/10.1007/s10584-016-1596-2.